306
10/3/79

DR. 111

HEDL-TME 79-23
UC 79, b, h

RESULTS FROM THE RUN-BEYOND-CLADDING-BREACH IRRADIATION OF A PREDEFECTED FUEL PIN (RBCB-6)

Hanford Engineering Development Laboratory

HANFORD ENGINEERING DEVELOPMENT LABORATORY
Operated by Westinghouse Hanford Company
P.O. Box 1970 Richland, WA 99352
A Subsidiary of Westinghouse Electric Corporation
Prepared for the U.S. Department of Energy
under Contract No. DE-AC14-76FF02170

NOTICE

Printed in the United States of America
Available from
National Technical Information Service
U.S. Department of Commerce
5285 Port Royal Road
Springfield, Virginia 22161
Price: Printed Copy $5.25; Microfiche $2.25

HEDL-TME 79-23
UC 79, b, h

RESULTS FROM THE RUN-BEYOND-CLADDING-BREACH IRRADIATION OF A PREDEFECTED FUEL PIN (RBCB-6)

Hanford Engineering Development Laboratory

D. C. Langstaff
M. Y. Almassy
D. F. Washburn

August 1979

HANFORD ENGINEERING DEVELOPMENT LABORATORY
Operated by Westinghouse Hanford Company
P.O. Box 1970 Richland, WA 99352
A Subsidiary of Westinghouse Electric Corporation
Prepared for the U.S. Department of Energy
under Contract No. DE-AC14-76FF02170

HEDL-TME 79-23
UC 79, b, h

RESULTS FROM THE RUN-BEYOND-CLADDING-BREACH IRRADIATION OF A PREDEFECTED FUEL PIN (RBCB-6)

D. C. Langstaff, M. Y. Almassy,
and D. F. Washburn

ABSTRACT

A slit was machined through the cladding of an irradiated fuel pin and irradiation in the Experimental Breeder Reactor-II (EBR-II) was resumed. The condition of the fuel pin was continuously followed with delayed neutron (DN) monitors. When the DN signal increased to a previously established administrative limit, the test was terminated. Postirradiation examination showed the sodium-fuel reaction caused fuel swelling and extension of the machined slit. There was no evidence of fuel loss nor was there any indication of impending pin-to-pin failure propagation. This test supports an increase in DN signal for subsequent run-beyond-cladding-breach (RBCB) tests.

ACKNOWLEDGMENTS

The authors would like to take this opportunity to express their appreciation and thanks to the many people who aided in the preparation, conduct, and examination of this irradiation test. In particular we would like to thank J. P. Bacca, R. D. Phipps, G. O. Haynor, and the HFEF/N cell operators who were responsible for machining the cladding slit, disassembling the subassembly, and aiding in fuel pin examination; J. I. Sackett and his staff at EBR-II for their concerted effort in obtaining the necessary approvals for irradiation of the test; Y. Harker and I. Steffan of EG&G Idaho, Inc., for their efforts in completing the fissile assay; J. D. Berger and T. T. Arey (HEDL) for their efforts in coordinating the activities at the Idaho National Engineering Laboratory; and L. A. Pember and his postirradiation testing laboratory staff for their diligence in conducting the destructive examination of the fuel pin.

CONTENTS

FIGURES

FIGURES (CONTINUED)

TABLES

I. SUMMARY OF RESULTS AND CONCLUSIONS

A fuel pin at a burnup of 7.8 atom percent (at.%) was defected by machining a slit through the cladding. The area of the slit was 0.19 cm^2. No attempt was made to seal the slit after machining. The predefected fuel pin was irradiated in the Experimental Breeder Reactor-II (EBR-II) for 8 hours at full power. During the power increase, the delayed neutron (DN) signal increased nonlinearly. Prior to irradiation it was decided that the test would be terminated when the DN signal increased by 120 counts per second (cps) at steady-state power. During steady-state irradiation the DN signal slowly but continuously increased until the administrative shutdown limit was reached.

Sodium-fuel reaction caused the cladding slit to extend in both directions; the final defect area measured 0.28 cm^2. There was no indication of fuel loss through the cladding defect. The test pin diameter increased less than 5%, and there was no indication of impending pin-to-pin failure propagation.

The fuel pin was shipped from the Hot Fuel Examination Facilities (HFEF) to the Los Alamos Scientific Laboratory (LASL) for betatron radiography and then to the Hanford Engineering Development Laboratory (HEDL) for destructive examination. An unsuccessful attempt was made to maintain an inert environment in the shipment tube. Consequently, there was a reaction between the environment and the sodium-fuel reaction product or unreacted sodium. This out-of-reactor reaction caused a large fuel pin diameter increase at the slit and the loss of some material through the slit. This occurrence points out the need for adequate protection of run-beyond-cladding-breach (RBCB) fuel pins to prevent undesirable alterations in fuel pin conditions.

Sodium-fuel reaction occurred over the entire fuel column length. The reaction was confined to a circumferential rim extending from the outer fuel surface to a depth of 0.7-0.9 mm.

The results of this test provided a measure of the sensitivity of DN signals to cladding crack size and showed that reaction-induced cladding crack extension is slow enough to allow reactor operators sufficient time to take the necessary action to avoid a potential safety hazard. There was no indication that any safety hazard was developing as a result of irradiation. The results from this test will be used to support higher DN signal limits during irradiation or subsequent RBCB tests.

II. INTRODUCTION

A series of run-beyond-cladding-breach (RBCB) tests was planned for the EBR-II to provide data to support the postbreach irradiation of mixed-oxide fuel pins in a sodium-cooled fast breeder reactor (FBR). The data required for this support include:

- The tendency for fuel loss through a cladding crack,
- The rate of fuel pin deterioration,
- The tendency for pin-to-pin failure propagation, and
- The ability of reactor instrumentation to monitor fuel in contact with coolant.

Without these data FBR operation would require immediate identification and removal of breached fuel pins, which would affect plant availability and economics.

Prior to initiating the RBCB irradiation test program in EBR-II, several safety and operational questions were resolved.[1,2,3] Delayed neutron monitors--the primary method for monitoring fuel exposed to coolant--were calibrated with a fission product source[4] and predefected UO_2 elements.[5]

RBCB behavior of cladding breaches that occur in-reactor are of major interest. However, it is difficult to evaluate these breaches because of the relative unpredictability of such naturally occurring end-of-life cladding breaches. In an attempt to alleviate this difficulty, defects were machined through the cladding of two irradiated mixed-oxide fuel pins. These defected fuel pins were irradiated individually in EBR-II until the test was terminated due to administrative DN signal limits. The tests were designed to satisfy two objectives:

- To obtain information on the in-reactor sodium-fuel reaction without having to wait for in-reactor breaches to occur and
- To provide calibration data for EBR-II fission-product monitors, especially DN detectors.

The first test of a predefected mixed-oxide fuel pin was designated RBCB-6; results from that test are described in this report. The RBCB-7 test is the second of the predefected fuel pin tests, and RBCB-1 through RBCB-5 identify planned tests of in-reactor breached fuel pins.

During the design of the predefected fuel pin tests, several features were recognized that could significantly affect the results of the tests. For example, a machined defect will not yield the same crack propagation results as an in-reactor cladding crack. Sodium ingress through a machined defect could be more extensive than through a crack, and fuel exposure to the hot-cell atmosphere (albeit inert) during machining could alter the sodium-fuel reaction.

In spite of these potential shortcomings, these tests provided a DN source for calibration of the DN detection system with mixed-oxide fuel, which allowed for less restrictive irradiation conditions for in-reactor breached pins. Moreover, the predefected pin tests provided an opportunity to develop and demonstrate handling procedures for fuel pins with exposed fuel.

III. TEST DESCRIPTION

A. FABRICATION DATA FOR FUEL PIN

Fuel pin ZP-8-24, the pin that was predefected for Test RBCB-6, originally contained 75% U-25% Pu mixed-oxide fuel in 5.84-mm (0.230-in.) outside diameter (OD) 20% cold-worked (CW) 316 stainless steel (SS) cladding with a 0.38-mm (0.015-in.) wall thickness. The fuel pin was 154.46 cm (60.81 inches) long. The uranium was 89% enriched in ^{235}U, and the oxygen-to-metal ratio (O/M) was 1.96. The pin geometry and dimensions are detailed in Figure 1. Additional design parameters are listed in Table 1.

B. PRIOR IRRADIATION HISTORY AND FUEL PIN CONDITION

Pin ZP-8-24 was irradiated in EBR-II starting in Run 75A. The fuel pin was included in the SLSF-1 (X224) subassembly (see Figure 2), which was a 61-pin subassembly containing mixed-oxide fuel pins of varied ^{235}U enrichments and nonfueled dummy pins. The subassembly was in the 6A2 core location throughout irradiation. The irradiation continued through EBR-II Run 83C when X224 was moved from the reactor core to the core basket. Burnup of pin ZP-8-24 was 7.8 at.%, and cladding fluence was 6×10^{22} neutrons/cm^{-2}. An irradiation summary is shown in Table 2.

Postirradiation examination at HFEF/N following the removal of X224 from the reactor showed that the pin was discolored and slightly bowed and that the wire wrap was loose. Neutron radiography revealed a normal fuel and insulator structure. There was a small central void in the lower one-third of the fuel column. The gross gamma scan shown in Figure 3 appeared normal. Spiral profilometry revealed no anomalies. The maximum pin diameter growth was less than 0.025 mm (0.001 inch).

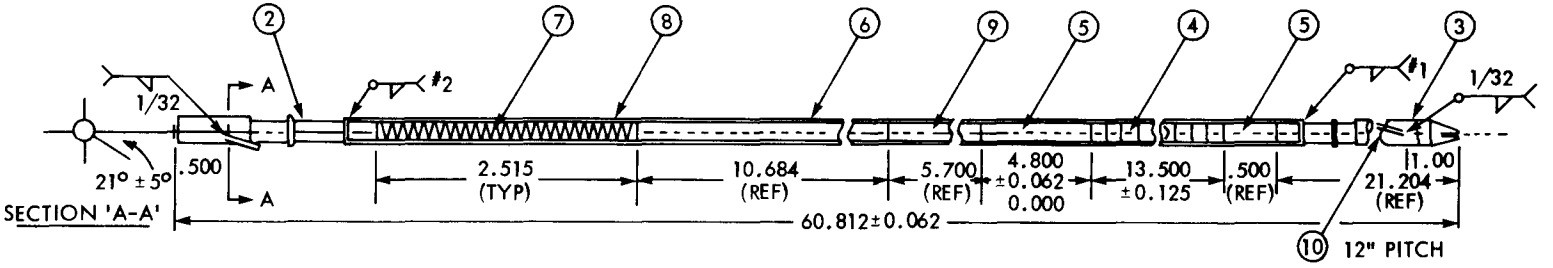

(1) ASSEMBLY

(2) END CAP (TOP)

(3) END CAP (BOTTOM)

(4) FUEL PELLET

(5) INSULATOR PELLET

(6) PLENUM SPACER

(7) SPRING-COMPRESSION

(8) TUBING $\begin{smallmatrix}5.85\text{ mm}\\5.83\text{ mm}\end{smallmatrix}$ OD X $\begin{smallmatrix}5.11\text{ mm}\\5.06\text{ mm}\end{smallmatrix}$ ID X $\begin{smallmatrix}97.07\text{ cm}\\96.98\text{ cm}\end{smallmatrix}$ LONG, 316 SS 20% CW

(9) REFLECTOR $\begin{smallmatrix}4.83\text{ mm}\\4.80\text{ mm}\end{smallmatrix}$ DIAM X $\begin{smallmatrix}14.52\text{ cm}\\14.44\text{ cm}\end{smallmatrix}$ LONG, INCONEL 600

(10) WIRE WRAP $\begin{smallmatrix}1.08\text{ mm}\\1.05\text{ mm}\end{smallmatrix}$ DIAM, 316 SS 20% CW

FIGURE 1. RBCB-6 Fuel Pin (ZP-8-24).

TABLE 1

FUEL PIN DESIGN PARAMETERS

Fuel	UO_2 - PuO_2
Fuel Composition Pu/Pu+U	0.250 ±0.009
Uranium Enrichment	89.0 ±1.0 wt.% ^{235}U in U
Plutonium Enrichment	88.0 ±0.5 wt.% ^{239}Pu + ^{241}Pu in Pu, 0.5 wt.% max ^{238}Pu 11.0 ±1.0 wt.% ^{240}Pu in Pu
Fuel Pellet Diameter	0.4940 cm ±0.0038 cm
Fuel Pellet Geometry	Dished Ends
Dish Depth	0.0089 cm ±0.0038 cm
Fuel Column Length	34.3 cm ±0.32 cm
Fuel Pellet O/M	1.960 ±0.020
Fuel Pellet Theoretical Density (TD)	10.92 g/cc
Fuel Pellet Density	90.4% TD 9.867 g/cc
Fuel Smeared Density	85.5 ±2.00% TD 9.332 g/cc ±0.22 g/cc
Fuel Column Weight	64.3 g ±3.5 g
Natural UO_2 Column (total length)	13.46 cm +0.208 or -0.051 cm
Cladding Material	316 SS
Cladding Condition	20% Cold Worked
Cladding Dimensions	0.5842 cm ±0.0013 cm OD x 0.5080 cm ±0.0013 cm ID x 97.025 cm ±0.041 cm long
Wire-Wrap Material	316 SS
Wire-Wrap Condition	20% Cold Worked
Wire-Wrap Diameter	0.1067 cm ±0.0013 cm
Plenum Spring Material	302 SS
Plenum Spacer Dimensions	27.137 cm ±0.051 cm long x 0.490 cm ±0.0076 cm diameter
Plenum Spacer Material	316 SS
Gas Plenum Volume (nominal)	6.1 cm^3
Plenum Gas	Helium + 1.0 ±0.2 cm^3 Xenon
Plenum Gas Pressure at Room Temperature	Atmospheric
Reflector Material	Inconel 600
Reflector Dimensions	14.48 cm ±0.038 cm long x 0.4813 cm ±0.0013 cm diameter
Reflector Volume (nominal)	2.63 cm^3

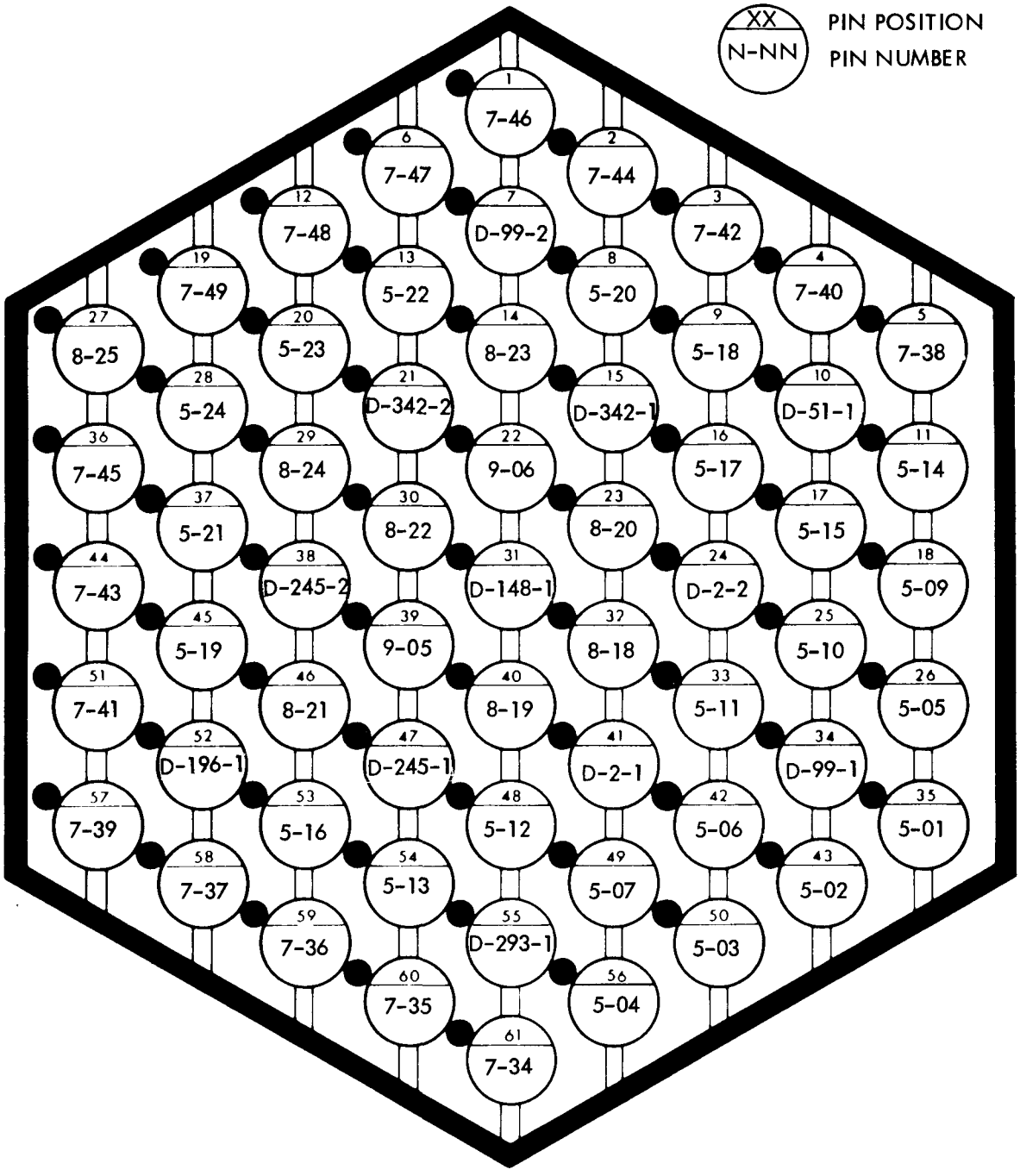

FIGURE 2. Loading Diagram for the SLSF-1 (X224) Subassembly. The RBCB-6 defected fuel pin (ZP-8-24) was from Position 29.

TABLE 2

END-OF-IRRADIATION SUMMARY FOR PIN ZP-8-24

Subassembly Name	SLSF-1
EBR-II Name	X224
Core Location	6A2
Ending EBR-II Run	83C

PEAK ENDING CONDITIONS

Cumulative Effective Full-Power Days	405.0
Burnup	7.8 at.%
Burnup	75,575.0 MWd/MTM
Fluence >0.1 MeV	5.09×10^{22} n/cm^2
Flux >0.1 MeV	1.45×10^{15} n/cm^2-s
Total Fluence	6.02×10^{22} n/cm^2
Total Flux	1.71×10^{15} n/cm^2-s
Gas Release %	96.7%
Gas Release	98.85 cm^3
Plenum Pressure	746.0 psig
Linear Heat Rating	281.0 W/cm
Coolant Temperature	539°C
Cladding OD Temperature	546°C
Cladding ID Temperature	570°C
Fuel Surface Temperature	961°C
Fuel Core Temperature	1758°C

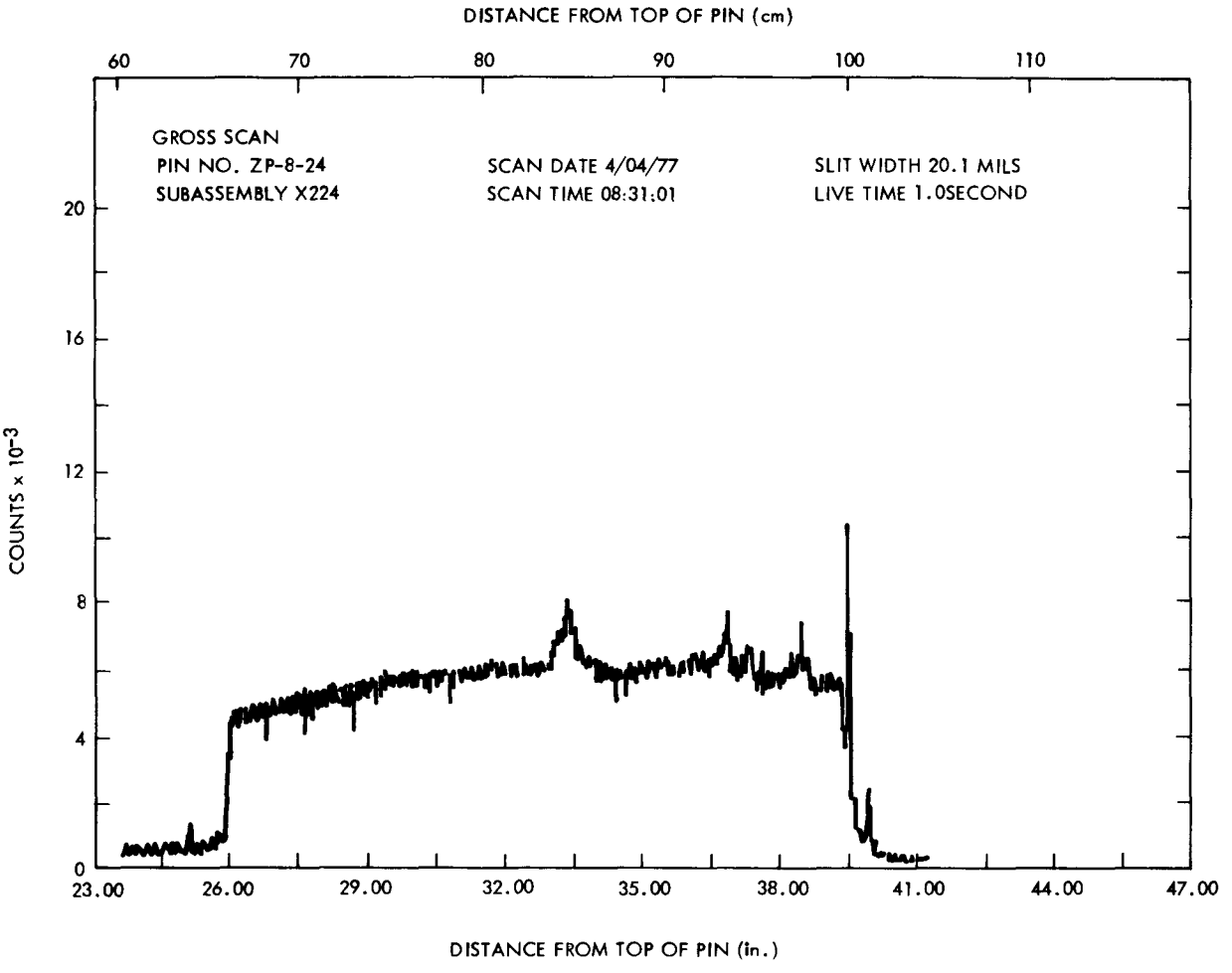

FIGURE 3. Gross Gamma Scan for Pin ZP-8-24 Prior to RBCB Irradiation.

C. DEFECTING PROCEDURE AND DEFECT APPEARANCE

The defect was centered about 30 mm (1 1/4 inches) below the top of the fuel column. This location was representative of the location of naturally occurring breaches and allowed a relatively long slit to be machined through the cladding and yet not extend beyond the fuel column.

A slitting saw was designed and built to slit the cladding of irradiated fuel pins,[6] and the irradiated fuel pin was defected by machining a slit through the cladding. Slit location and length could be controlled, but slit width was dictated by the cutting wheel width. The slitting machine used a readily

available diamond-impregnated cutting wheel, required no blade coolant, did not contaminate the fuel or fuel pin, and limited the spread of radioactive particles in the hot cell during the remote cutting operation.

The fuel pin was oriented so that the slit was opposite the wire wrap. The slit was 21-mm (0.82-in.) long by 0.61-mm (0.024-in.) wide and was centered 30 mm (1 1/4 inches) below the top of the fuel column. Good fuel exposure was observed along the bottom of the slit as shown in Figure 4. The slit was machined in the inert atmosphere of HFEF/N. No attempt was made to plug the defect after it was machined.

FIGURE 4. As-Machined Cladding Defect Showing the Good Fuel Exposure at the Bottom of the Slit.

D. SUBASSEMBLY LOADING

The RBCB-6 (X309) subassembly was loaded at HFEF/N using MK-E-37D subassembly hardware. All fuel pins in X309 were previously irradiated in X224 except for two unirradiated pins (ZP-5-26 and ZP-5-51). Fuel pins in the subassembly were located to minimize fuel pin bow effects (see Figure 5). No problems were encountered during the loading operation. The hexagonal duct was lowered over the fuel pin bundle with little resistance and was welded to the lower spool piece. The subassembly was placed in the HFEF/N storage pit until it was inserted into EBR-II. Sodium ingress probably occurred immediately upon insertion into EBR-II.

The RBCB-6 subassembly was irradiated in Position 6A2 of EBR-II during Run 89A. The peak pin power for the predefected fuel pin (ZP-8-24) was 297 watts/cm. The sodium flow rate through the subassembly was 3.20 lbm/s. Burn-up and fluence accumulation during RBCB-6 irradiation was minimal because the test was terminated after only 8 hours at full power.

E. TEST TERMINATION CRITERION

A test termination criterion was established based on the DN signal from the fuel element rupture detection (FERD) system. A DN signal limit was set that would require a manual scram of the reactor. In setting this limit it was assumed that particulate fuel would be released through the slit, that the fuel particles would form a coolant channel blockage in the core region,[7] and that the release of DN precursors per unit surface area of particulate fuel would be the same as that from the UO_2 test. An analysis based on these assumptions indicated that coolant channel blockage would produce a signal of at least 120 counts per second (cps). Therefore, the DN limit for RBCB-6 was set at 120 cps above the DN signal when the reactor first reached full power. A signal above this limit would require a manual reactor scram and termination of the test.

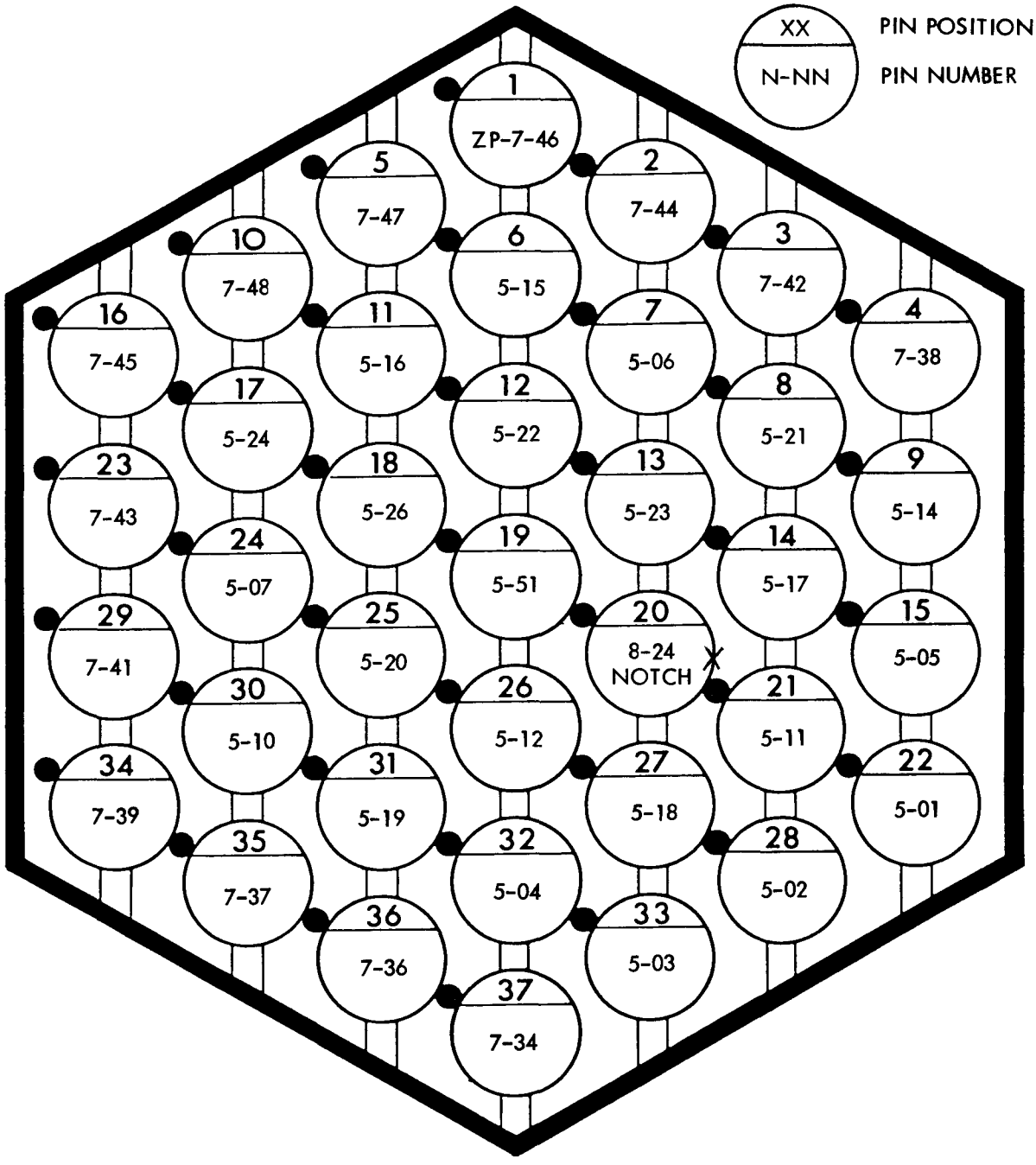

FIGURE 5. Loading Diagram for Test RBCB-6. "X" indicates the notch orientation. The black circles represent the wire-wrap locations in the assembly (not necessarily at the defect height).

IV. RBCB-6 IRRADIATION HISTORY

The change in the average DN signal during the rise to power is shown in Figure 6. The rapid increase in the DN signal beyond 30 MW power was not expected, and as a result there were several "holds" at intermediate power levels to insure that the DN signal increase was due to power increase rather than to increased exposed fuel area. Each of these holds was several minutes long; therefore, the results shown in Figure 6 were obtained by averaging the signal over a 12-minute period. (DN signal data were recorded at the rate of 2 points per second.)

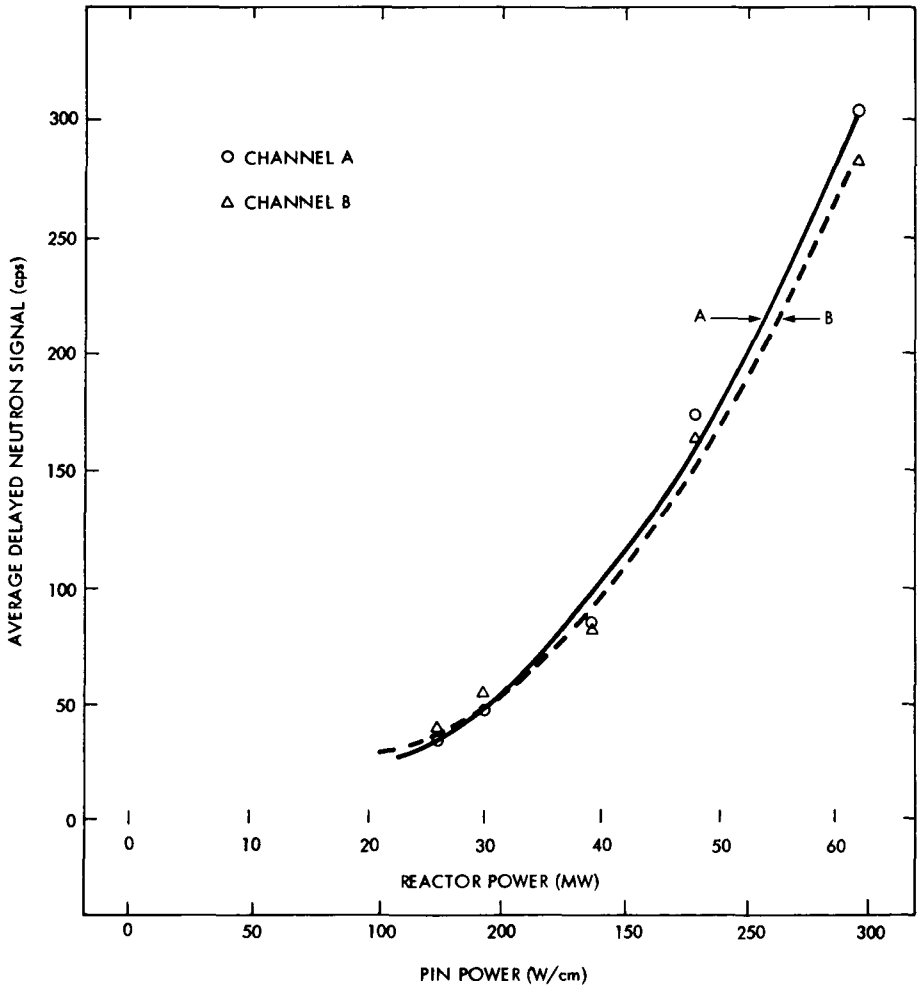

FIGURE 6. DN Signal from Test RBCB-6 (increased linearly with reactor or fuel pin power).

During the holds at constant power the DN signal remained fairly constant suggesting that the rapid increase in DN signal was related to the power change and a nonrecoil source rather than to a rapidly increasing defect area. After reaching full power (62.5 MW), the alarm settings of the FERD system were set at ∿120 cps above the peak DN signal. Alarm settings on the three FERD channels were: Channel A - 550 cps; Channel B - 530 cps; and Channel C - 520 cps. Normal background for these channels was about 50 cps. These alarm settings were all based on peak values.

During operation at full power (62.5 MW) the DN signal continued to increase gradually as shown in Figure 7. The curves in Figure 7 were obtained by averaging DN data, recorded at a rate of 2 points per second, over 5-minute intervals. (Only Channels A and B are shown since Channel C closely followed Channel B.) The alarm settings on FERD were reached on Channels B and C 7.5 hours after reaching full power and a manual scram was initiated.

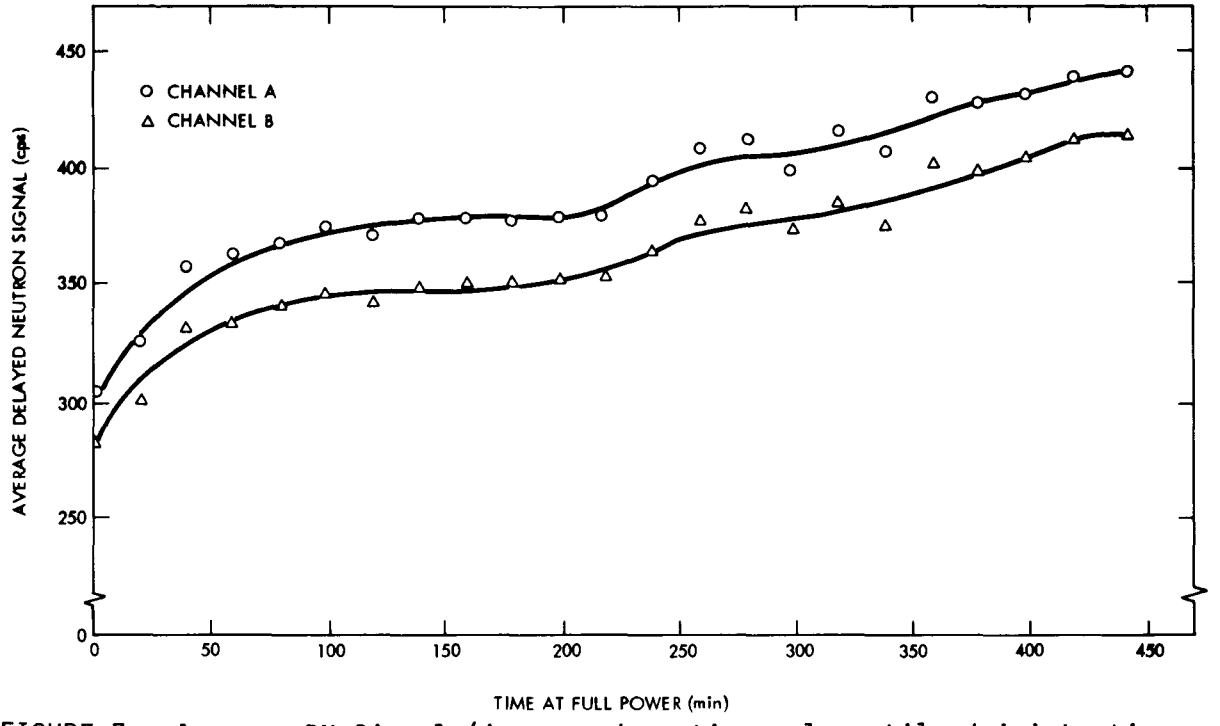

FIGURE 7. Average DN Signal (increased continuously until administrative shutdown limit was reached).

The only previous EBR-II experience with fuel directly exposed to the coolant were tests with metal fuel and tests with previously unirradiated UO_2. Neither of these tests had shown any change in DN signal while the reactor was at constant power although DN signals significantly above background were obtained. The DN signal with 0.2 cm^2 unirradiated UO_2 exposed to the coolant was about 120 cps, or 70 cps above background.

Fission gas release from RBCB-6 caused a significant increase in cover gas activity. The activity from the short-lived isotopes appeared to reach equilibrium shortly after full power was attained although the ^{138}Xe (14.2-minute half-life) gradually decreased during full-power operation.

The RBCB-6 subassembly was transferred from the reactor to HFEF/N in the interbuilding coffin (IBC) without forced cooling and without washing. Decay heat calculations by EBR-II indicated that because of the brief irradiation the transfer could be made in stagnant argon without exceeding 427°C (800°F) cladding temperature. The blowers in the IBC were not used during the transfer to avoid possible contamination of the IBC. Inspection of the IBC after the transfer did not reveal any indication of contamination from the RBCB-6 subassembly.

V. POSTIRRADIATION EXAMINATION

A. SUBASSEMBLY DISMANTLING

The potential for contamination dispersal by flowing argon was investigated using the filter shown in Figure 8, which was designed by HFEF/N personnel and installed at the vertical assembly-disassembly (VAD) machine. Argon flowing at a typical subassembly cooling rate was forced into the top of the subassembly and exhausted from the bottom through a 10-micron filter. Argon effluent was filtered for 4 hours; after which the filter was analyzed for Pu.

Results of this analysis showed there would be no significant spread of plutonium contamination from the subassembly during forced cooling. This result provides support for using forced cooling during RBCB subassembly transfers with higher decay heat.

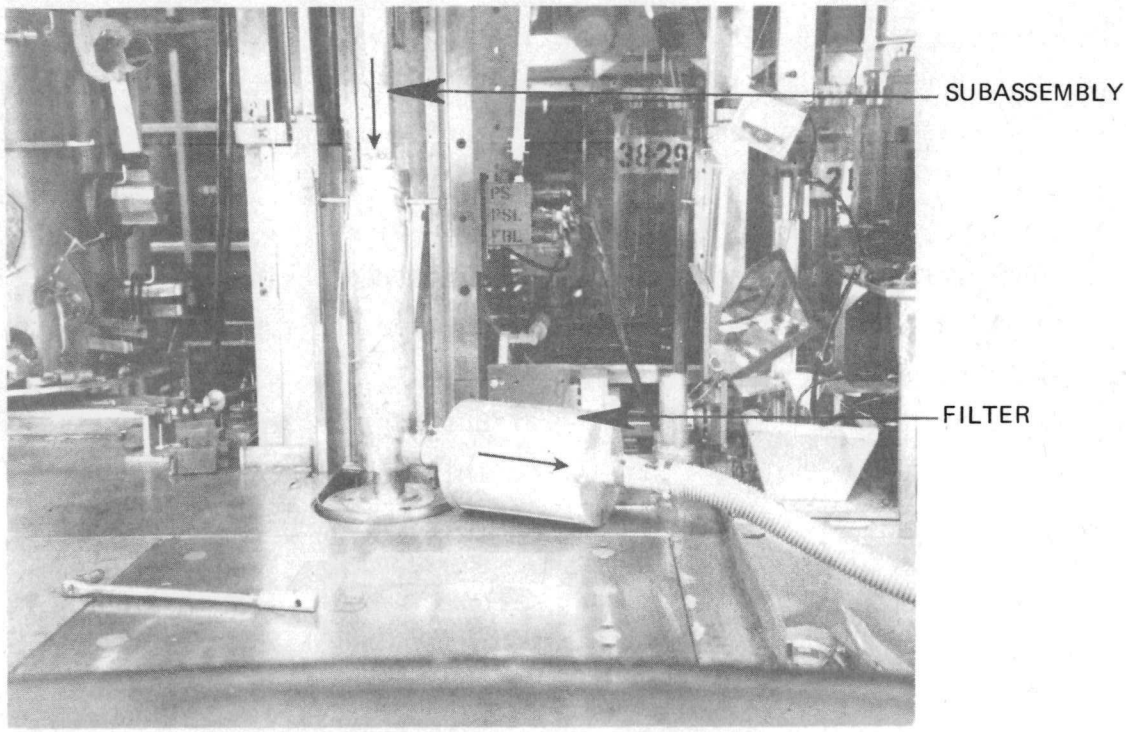

FIGURE 8. VAD Filter Installed to Investigate Potential Spread of Pu Contamination from RBCB Subassembly During Forced Cooling.

At the conclusion of the filtering operation, the hex can was separated from the spool piece. A force of 1100 lb was required to begin hex can removal; the removal force never exceeded 60 lb, with a nominal force of about 20 lb. Immediately after the hex can was removed, the sodium in the pin bundle had a metallic appearance. After about an hour, the sodium had developed a whitish appearance, indicating surface oxidation. The fuel pins had a dark appearance from the bottom up to about 1/2 inch above the lower end cap weld. Above the dark area, the cladding was bright metallic but dulled at the fuel midplane and above.

The pin bundle was straight immediately after the hex can was removed. However, after the first few pins were removed from the grid, the pin bundle "bird-caged" showing the bow typical of an irradiated subassembly. The residual sodium between pins appeared to hold the pins together in a straight configuration until the first few pins were removed.

Nothing unusual was observed in the pin bundle. The intentionally defected pin (ZP-8-24) was easily identified while in the bundle. Slit extensions were observed at each end of the slit. There was no evidence of fuel loss nor any indication of existing or impending coolant channel blockage.

After disassembly, smears were taken from several pieces of equipment to determine whether plutonium contamination had occurred during transfer and handling of the X309 subassembly. Smears taken from the fuel unloading machine, the IBC, and the subassembly exterior indicated no plutonium contamination. Levels up to 50,000 disintegrations per minute (dpm) were found on isolated portions of the VAD after subassembly dismantling.

After pin ZP-8-24 was removed from the subassembly, smears were taken from about 3-in. lengths of the cladding at seven axial locations. The locations and results from these smears are shown in Figure 9. Absolute levels for alpha (fuel), beta-gamma, and gamma (fission product) contamination have little significance in themselves since the areas of the smears were not closely controlled.

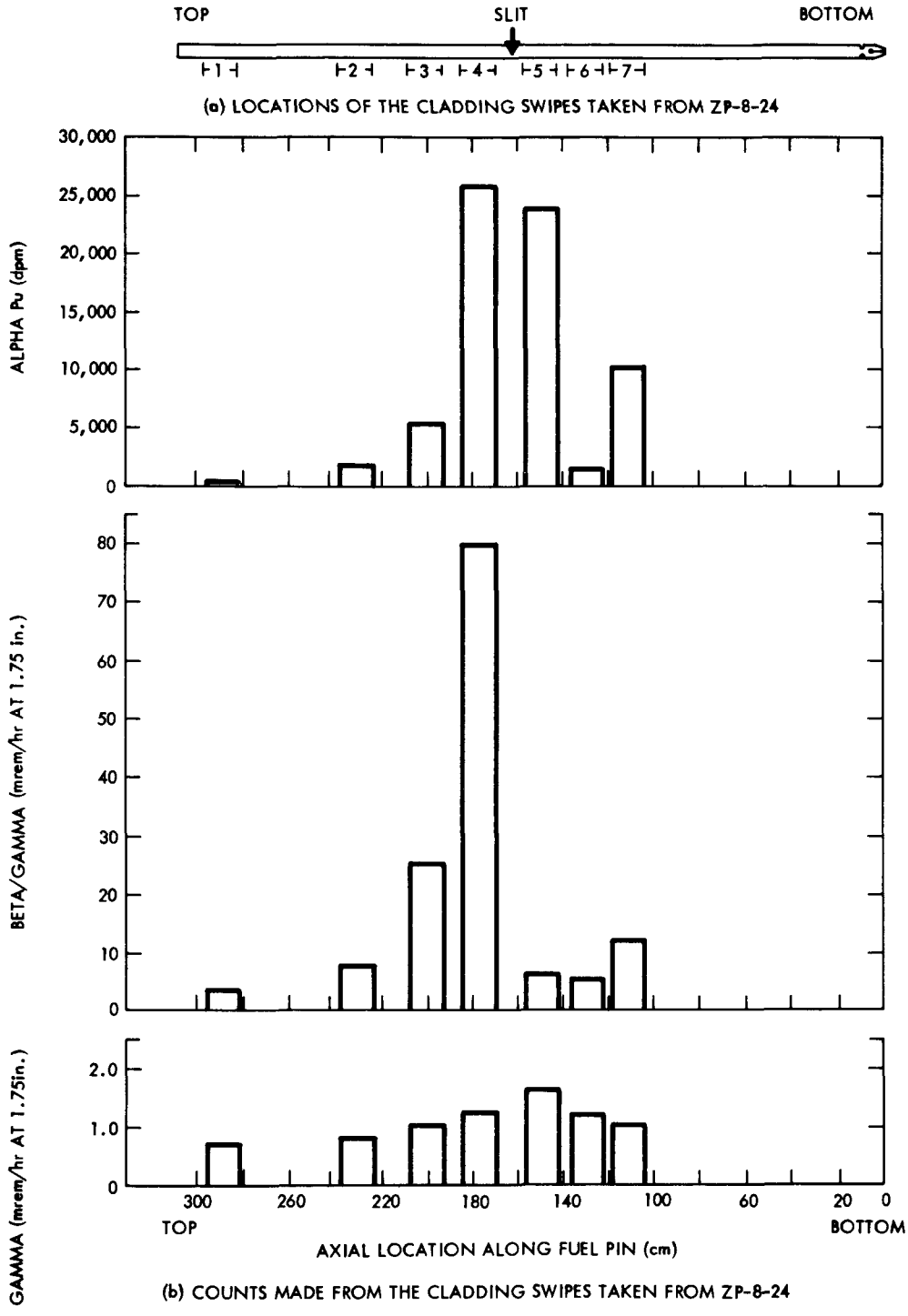

FIGURE 9. HFEF In-Cell Smear Survey Data Taken from ZP-8-24 After RBCB Irradiation.

Fuel and fission product contamination levels were highest adjacent to the breach and decreased rapidly with distance from the breach. The exceptions to this behavior were the two higher readings from the seventh smear for alpha and beta-gamma contamination. Conceivably this could be due to transport of fuel and/or fission products down the pin in a sodium droplet after the pin was removed from the reactor.

B. VISUAL EXAMINATION

Visual examination of the predefected fuel pin showed that the slit had extended equally upward and downward. Initial and final dimensions of the defect are shown in Table 3; final appearance of the defect is shown in Figure 10. The total area of the defect increased from 0.19 cm^2 to 0.28 cm^2--an increase of 47%.

What appeared to be sodium-fuel reaction product was still below the surface of the cladding, and there was no evidence of fuel release. Other than the extension of the machined slit, there was no other visible effect of RBCB irradiation. Careful examination of neighboring pins, especially the one facing the slit, showed no evidence of RBCB irradiation.

TABLE 3

DIMENSIONS OF THE RBCB-6 CLADDING DEFECT

	Before RBCB Irradiation	After RBCB Irradiation
Width	0.61 mm	0.79 mm
Length	2.08 cm	6.17 cm
Area	0.19 cm^2	0.28 cm^2

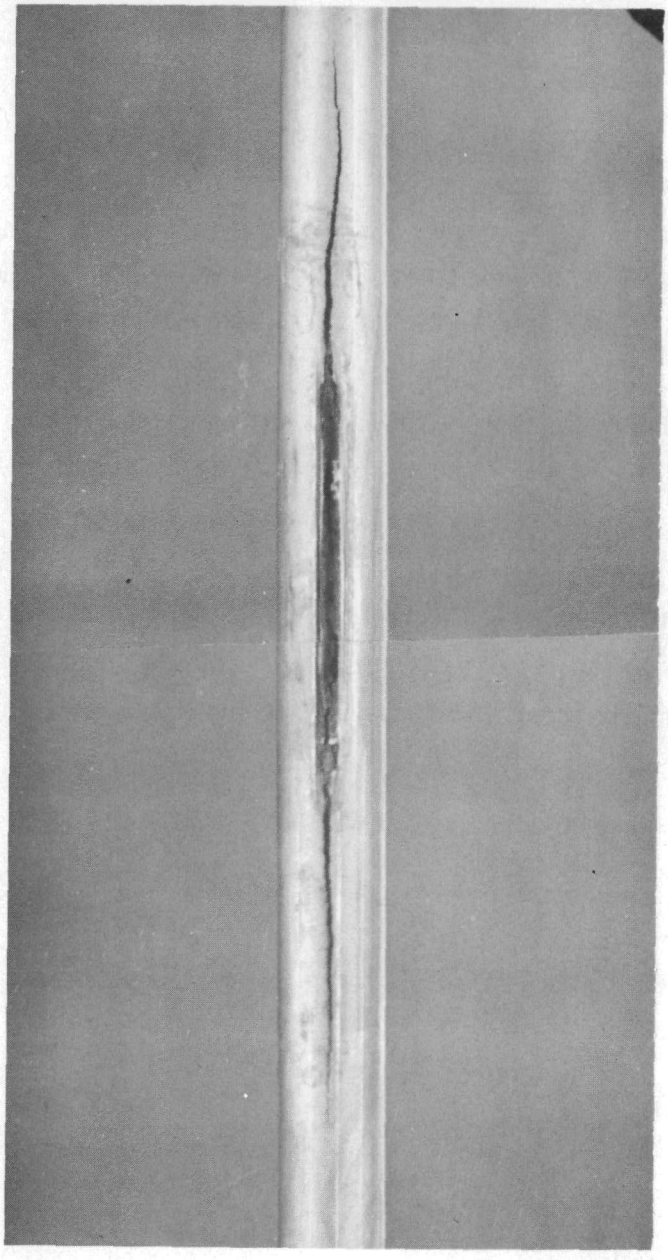

FIGURE 10. Final Appearance of the Defect. The only visible effect of R irradiation was the upward and downward extension of the slit

C. GAMMA SCAN

Comparison of pre- and post-RBCB irradiation gross gamma scans indicated that fuel pellet separations that were present initially were much less evident after RBCB irradiation. The gamma scans showed no change in fuel column length resulting from RBCB irradiation. The reduction of fuel pellet separation is attributed to the formation of sodium-fuel reaction product.

Enlarged plots of HFEF data from fuel pin gross gamma activity showed little or no difference between pre- and post-RBCB irradiation. Two post-RBCB gross gamma scans, which were taken at HFEF, showed no decrease in gamma activity near the top of the fuel column, indicating that there was no significant loss of fuel during RBCB irradiation. However, isotopic gamma scan data showed that a gradual depletion of ^{137}Cs over the top two-thirds of the fuel column took place during RBCB irradiation (see Figure 11).

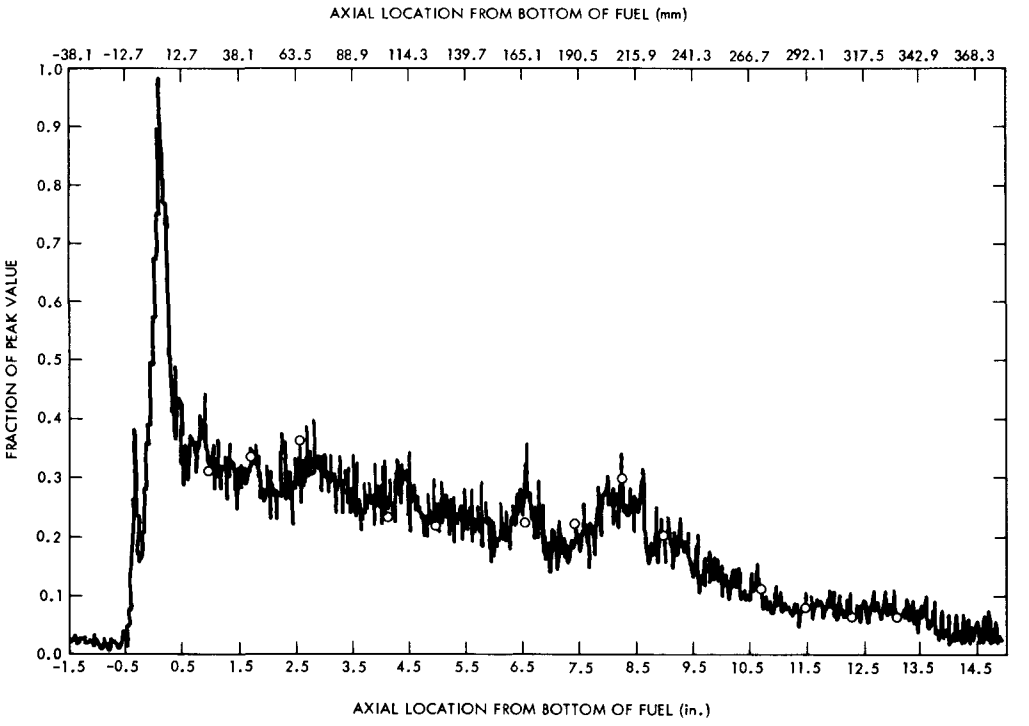

FIGURE 11. Cesium Gamma Scan for Pin ZP-8-24 After RBCB Irradiation (HEDL data).

D. FISSILE ASSAY

A fissile assay technique[8] was developed by EG&G Idaho, Inc., at the Advanced Reactivity Measurement Facility (ARMF) to determine fuel losses from RBCB fuel pins. Two fissile assay standards pins (one fueled and one dummy) were used to obtain a relationship between measured reactivity and mass of fissile material.

To perform a fissile assay each pin is encapsulated in a transfer tube and individually examined in ARMF. The encapsulated pin is lowered into a dry hole that extends through the ARMF-I reactor core by a cable and winch assembly. The reactor is brought to a low power level; the assembly is raised in increments by the winch assembly; and the reactivity worth of the test assembly is determined at each increment.

Reactivity worth of the test assembly is measured by observing the angular position of a rotating regulating rod. The test pin area exposed to the neutron flux in the core is fixed during the test. A servo-balancing mechanism maintains the reactor exactly critical at a low, constant power level by changing the angular position of the rod, which has been calibrated in terms of reactivity worth.

Reactivity profiles determined for the predefected irradiated fuel pin (ZP-8-24) after defecting and again after subsequent irradiation are shown in Figure 12. The scatter in the data made it difficult to discern the effect of RBCB irradiation; therefore, a statistical analysis was performed to determine whether the pre- and postirradiation profiles were statistically the same. Using the student's "t" test, the hypothesis that the pre- and postirradiation means were the same could not be rejected. This implied that there was no net change in fuel content over the length of the fuel column during RBCB irradiation.

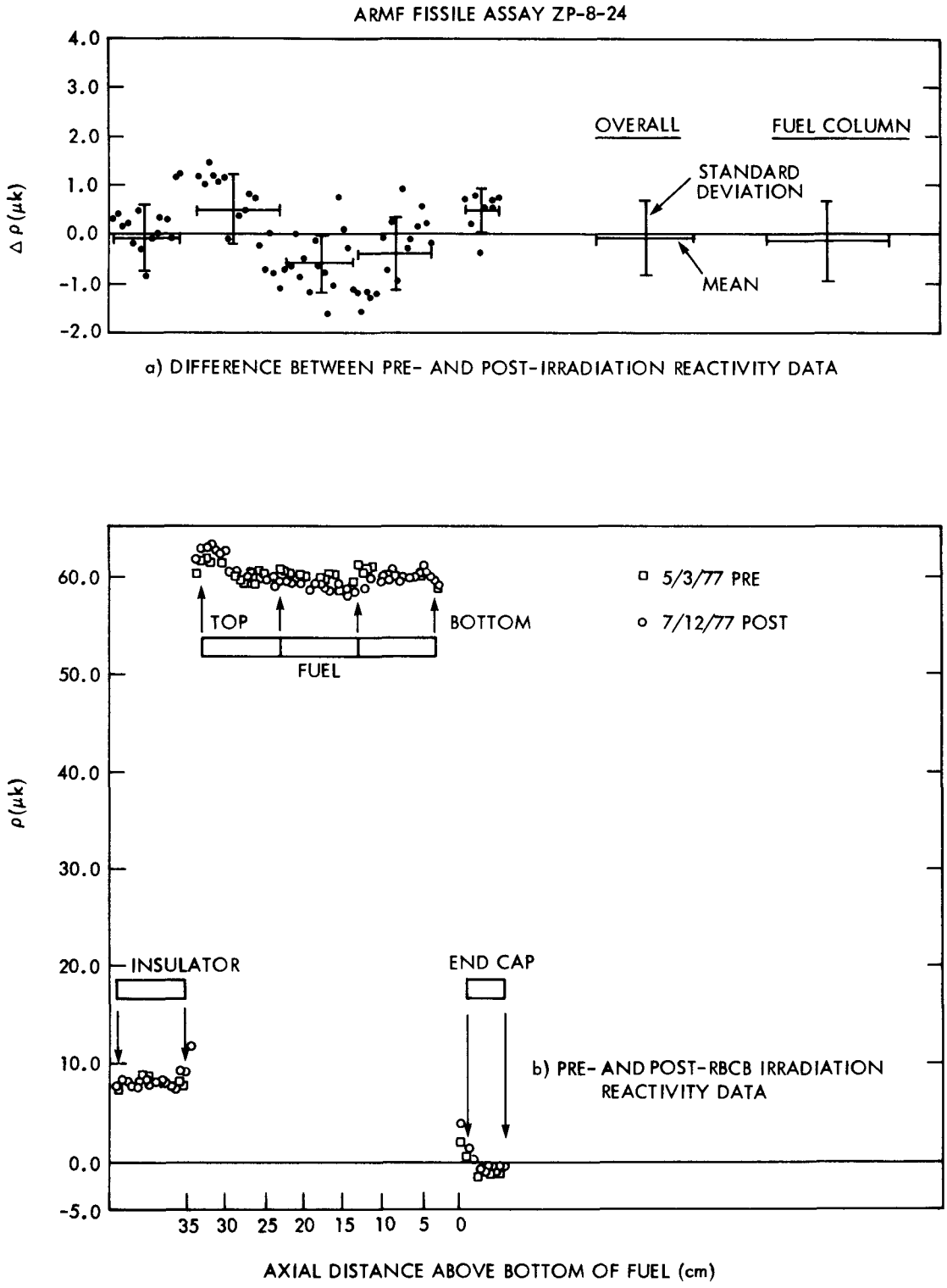

FIGURE 12. Fissile Assay Reactivity Data for Test RBCB-6 (ZP-8-24).

Evaluation of these and other data from irradiated fuel pins suggests that fuel column end effects, fuel composition, burnup, and presence of fission products may affect reactivity measurements. If so, these factors may limit the sensitivity of the technique. Analysis of reactivity data from several fuel pins is being conducted by EG&G Idaho, Inc., to resolve the effect of other variables on the measured reactivity.

E. FUEL PIN SWELLING

Pre- and post-RBCB irradiation diameters for pin ZP-8-24 are shown in Figure 13. The localized diameter increase of 4.9% was near the center of the as-machined slit and was due to RBCB irradiation. The pre-RBCB diameter prior to machining the slit was about 5.85 mm or 0.2% greater than the as-fabricated diameter, and the neutron-induced cladding swelling (as determined from density measurements) was less than 0.01% ($\Delta V/3V \times 100$). Machining the slit in the cladding may have allowed relaxation to occur, which would affect the final pin diameter. No attempt was made to measure the pin diameter after the slit was machined, but the effects of relaxation on pin diameter are expected to be negligible. The net increase in pin diameter during RBCB irradiation was attributed to the effects of the sodium-fuel reaction.

The diameter change at the ends of the slit extension provided an indication of the strain required to cause crack extension. An estimate of the cladding strain for crack extension from this fuel pin is 0.7%.

F. BETATRON RADIOGRAPHY

Betatron radiography was conducted at LASL to determine the structural integrity of the fuel after RBCB irradiation and to see if the extent of fuel loss could be estimated using radiographic techniques.

The pin was radiographed with the beam directly toward the breach (see Figure 14) and with the beam perpendicular to the breach (see Figure 15). Stereoscopic pairs of radiographs were taken in each orientation to facilitate visual interpretation of the radiographs.

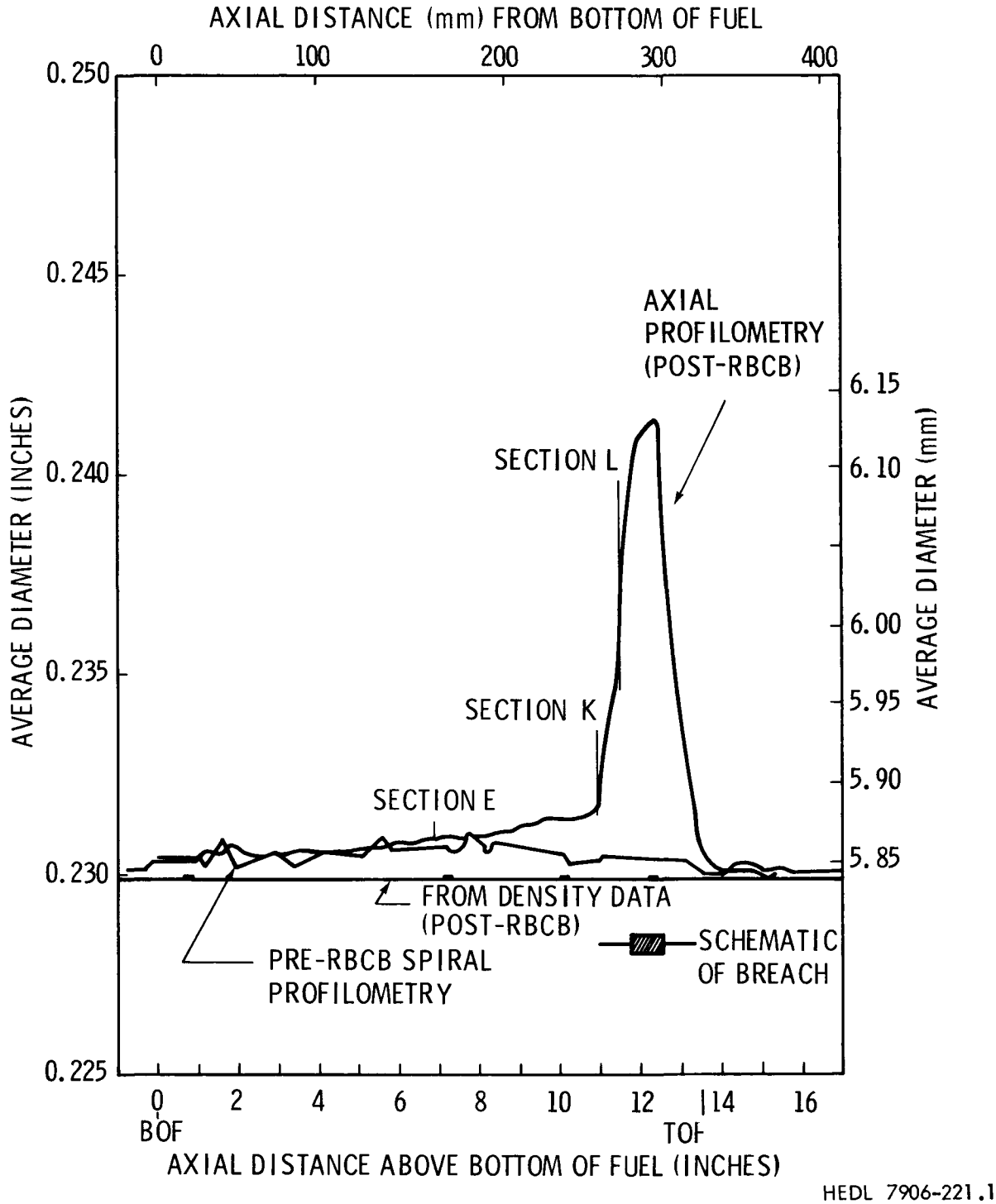

FIGURE 13. Diameter of RBCB-6 Fuel Pin Before and After RBCB Irradiation.
Neg 7908107-1

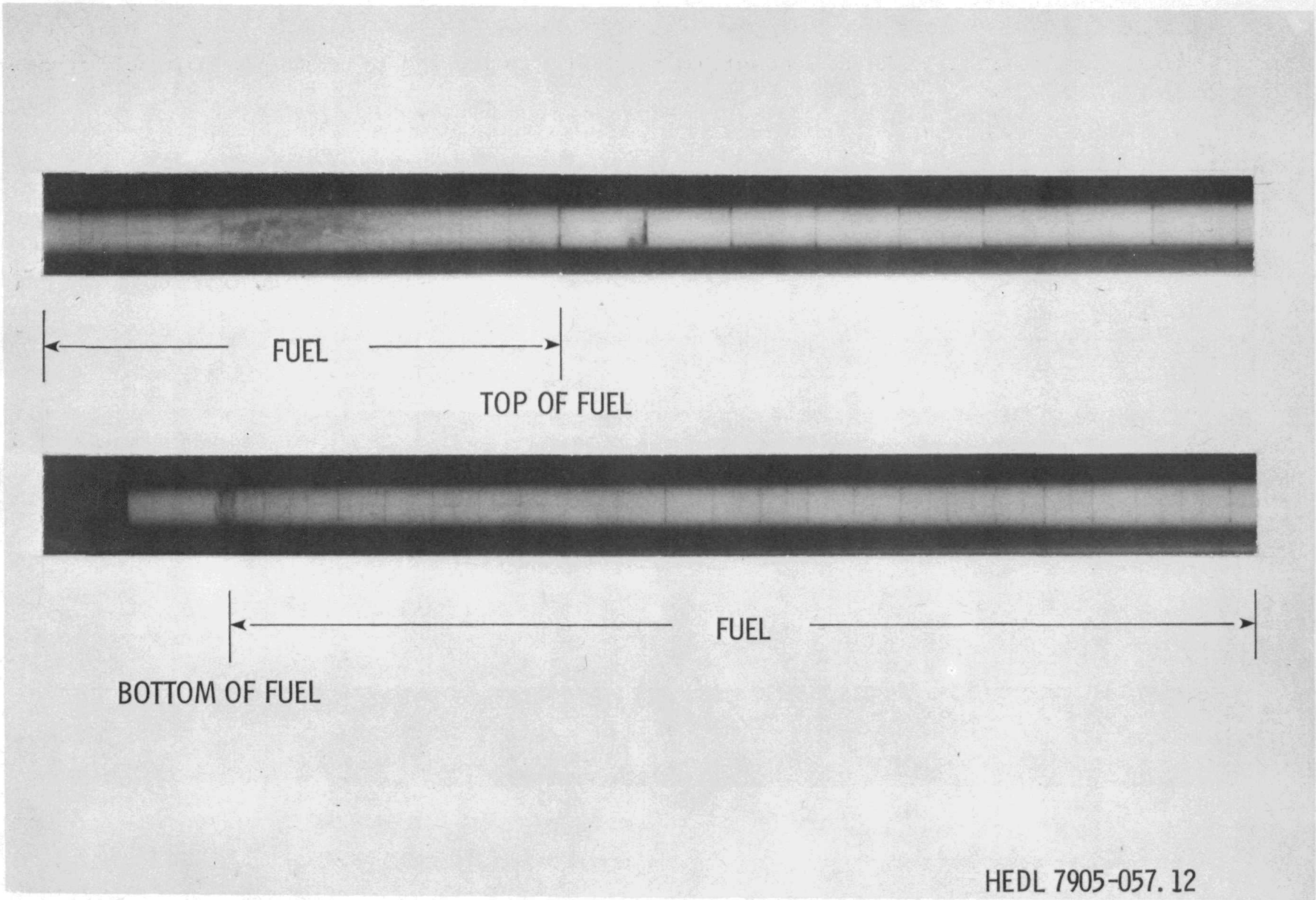

FIGURE 14. Betatron Radiograph of Pin ZP-8-24 After RBCB Irradiation Looking Directly at the Breach.

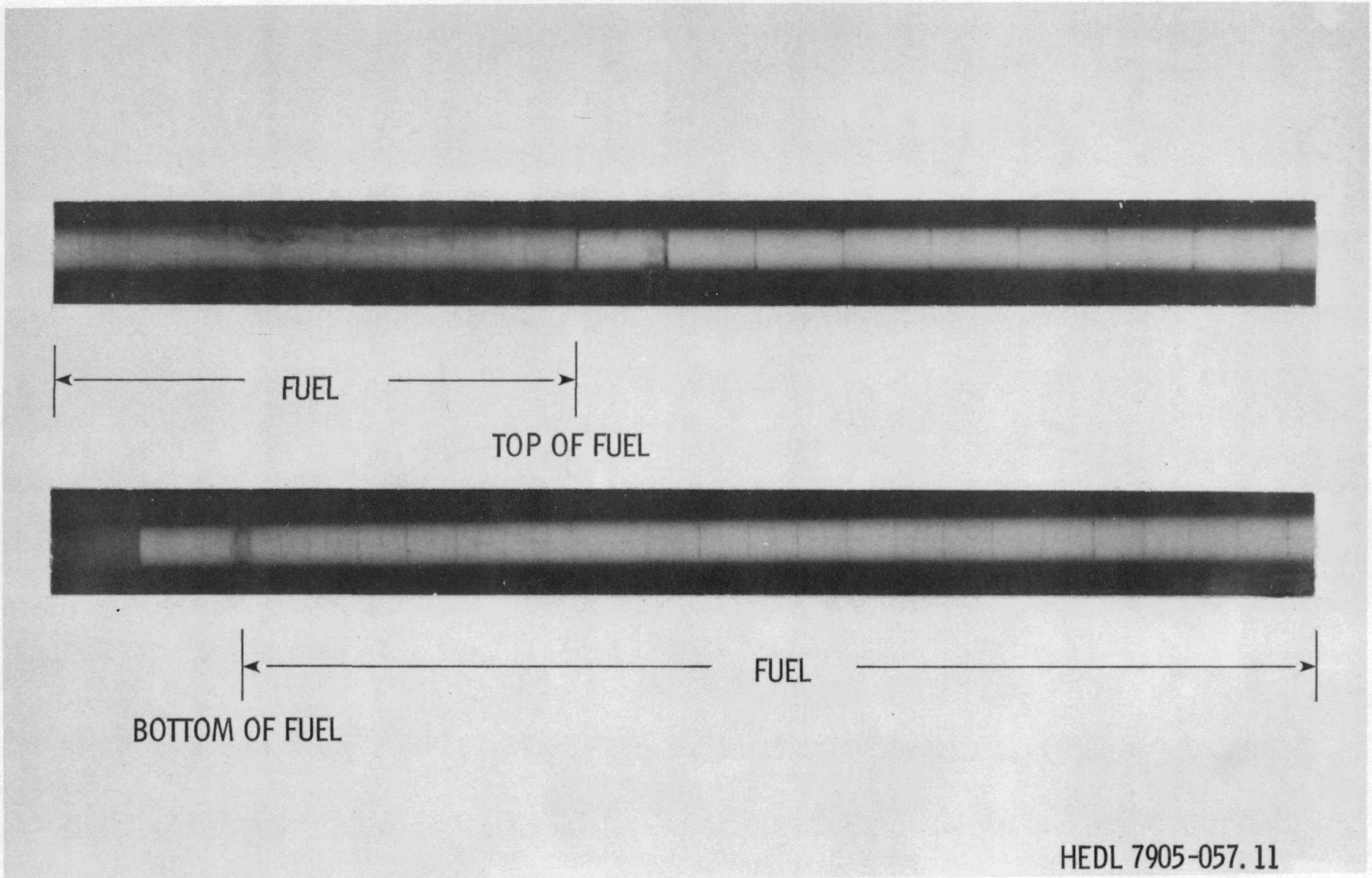

FIGURE 15. Betatron Radiograph of Pin ZP-8-24 After RBCB Irradiation Looking at the Breach Profile.

Structural irregularities in the fuel and insulator pellets were clearly evident from the radiographs. A large chip left a void when it came out of the top corner of the first upper insulator pellet; this observation was later verified by destructive examination. Neutron radiographs prior to RBCB irradiation revealed no structural defects in that pellet. Extensive reaction between sodium or cesium and fuel at the bottom fuel pellet-insulator interface was evident and was later confirmed by destructive examination. An area of decreased fuel density was coincident with the area of the cladding slit and slit extensions. This region of low density may have been due to sodium-fuel reaction product formation or to loss of fuel. To use betatron radiography for estimating fuel loss would require additional calibration to differentiate between sodium-fuel reaction and fuel loss.

G. FUEL PIN SHIPMENT

The defected fuel pin was shipped from HFEF to LASL and then to HEDL in a closed tube that was designed to prevent the spread of alpha contamination and maintain an inert environment. Figure 16a shows the pin defect region as it appeared at HFEF/N; Figure 16b, as it appeared at LASL; and Figure 16c, as it appeared at HEDL.

When the pin was removed from the tube at LASL for radiography, several unexpected observations were made. First, there was a highly gamma-active deposit on the inside wall of the tube at the axial height of the defect. Second, the cladding defect had widened appreciably. Third, a blister-like deposit covered the lower third of the slit. There is a possibility that the tube was not thoroughly cleaned or that the seal did not maintain an inert environment within the tube. In any event, it is obvious that care must be taken to protect exposed sodium-fuel reaction product.

The pin was placed in a new tube for shipment to HEDL. During shipment from LASL to HEDL or during handling at LASL the blister-like deposit was broken and some material was lost.

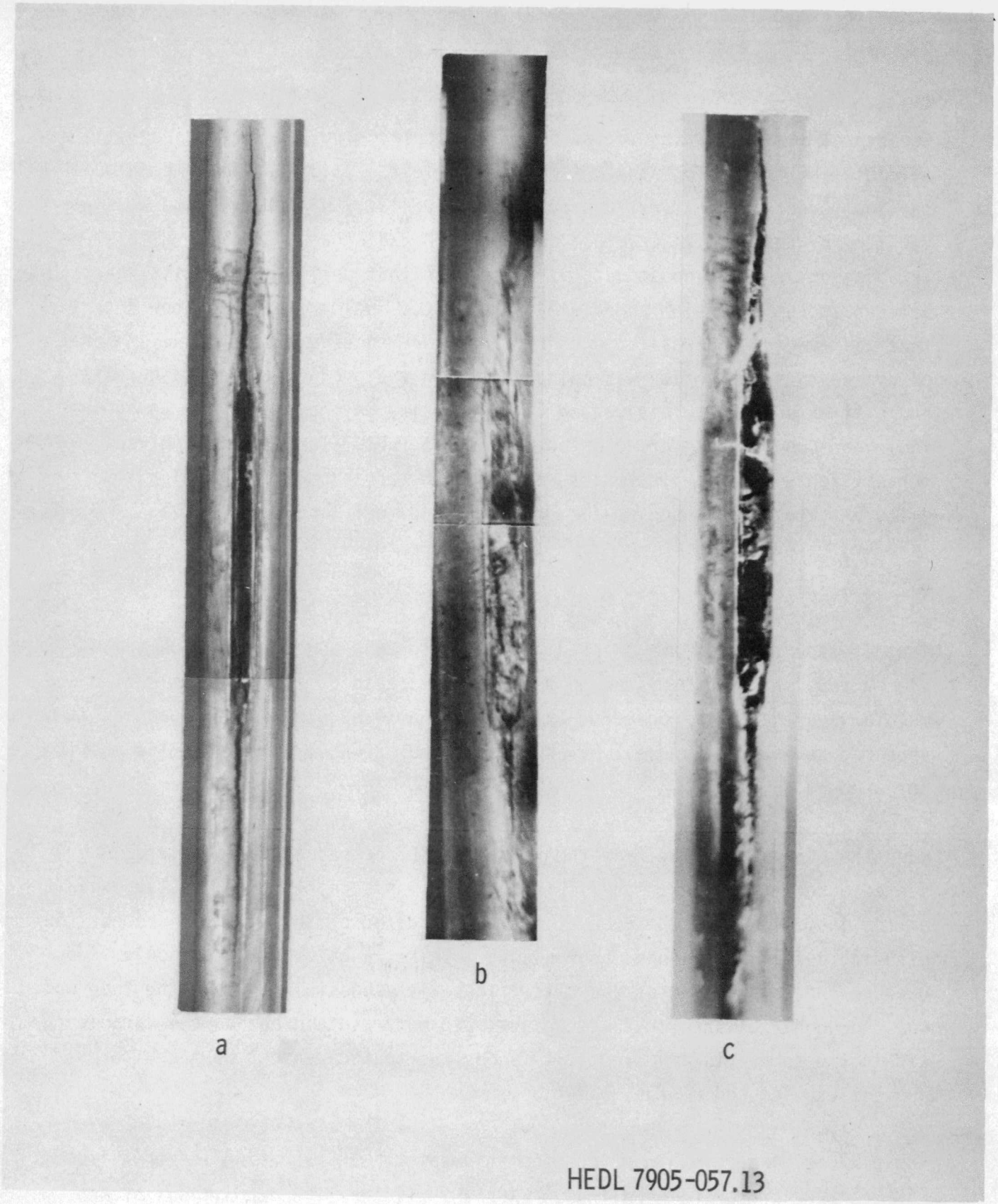

FIGURE 16. Cladding Breach Appearance During Initial Examination at a) HFEF/N, b) LASL, and c) HEDL.

Prior to sectioning the pin for destructive examination, diameter measurements were made at selected axial heights in the vicinity of the cladding defect. The results of these measurements are shown in Figure 17. Agreement between axial profilometry measurements (HFEF) and diameter measurements (HEDL) away from the defect is excellent and serves to confirm that the large diameter change in the slit region occurred during shipment. This diameter change was attributed to reaction between the environment and sodium-fuel reaction product or residual, unreacted sodium.

H. MICROSTRUCTURAL OBSERVATIONS

Pin ZP-8-24 was sectioned to provide five ceramography samples, five cladding density samples, and the fracture surface of the upper slit extension. The five cermographic sections were obtained from positions along the entire fuel column, including the top and bottom UO_2 insulators as shown in Figure 18. Because of the reaction that occurred during pin shipment, fuel microstructure in the middle of the machined slit no longer represented the in-reactor pin condition; therefore, this region was not examined in detail.

The three transverse sections--Figures 19, 20, and 21--and the two longitudinal sections--Figures 22 and 23--showed an outer ring of fuel that contained a distinct and nearly continuous grain boundary phase presumed to be sodium-fuel reaction product. During shutdown, this layer, which was estimated to have a maximum thickness of 0.75 mm (0.03 inch), was separated from the inner fuel core by a circumferential crack. The outermost surface of the fuel (to a depth of several microns) was almost completely reacted with sodium and had a structureless appearance. A grain boundary phase that gradually increased in width toward the center of the fuel existed below the outermost surface. The widest part of the grain boundary phase occurred at the circumferential crack. There was little, if any, sodium-fuel reaction inward from the circumferential crack.

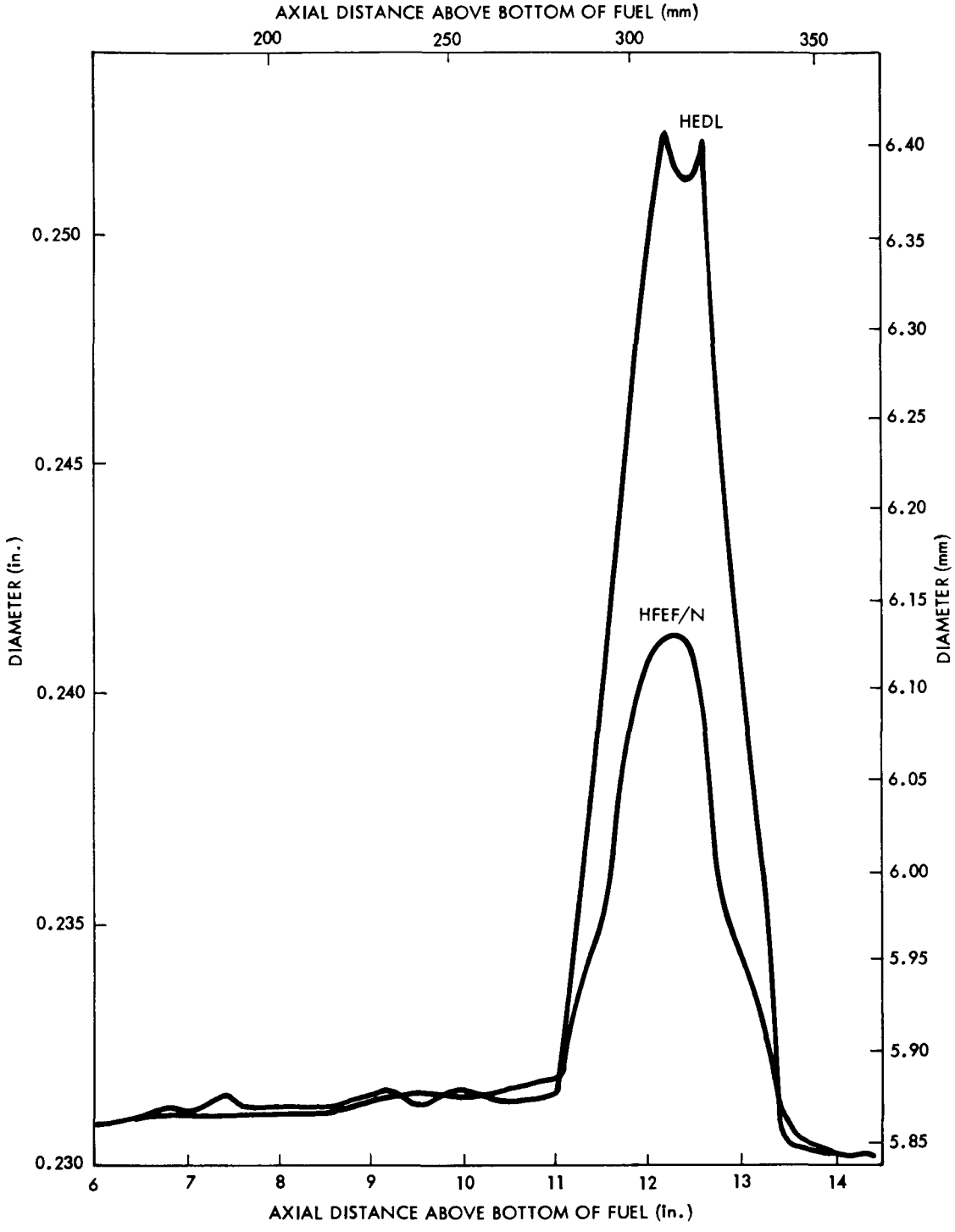

FIGURE 17. Profilometry of RBCB-6 Fuel Pin Showing the Diameter Changes That Occurred During Shipment from HFEF to HEDL.

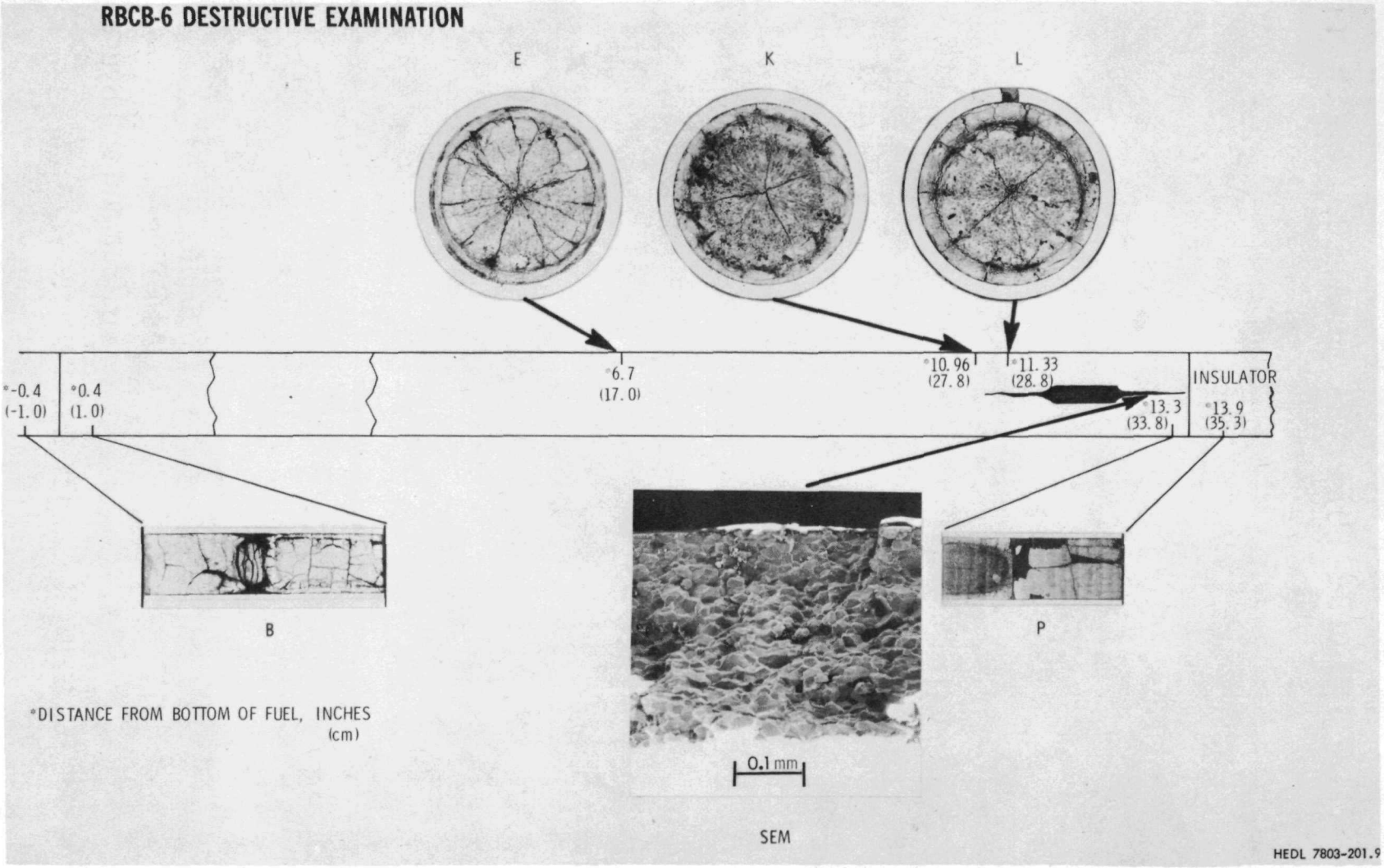

FIGURE 18. Summary of the Photomicrography from Pin ZP-8-24.

MIXED OXIDE FUEL IRRADIATED IN EBR-II

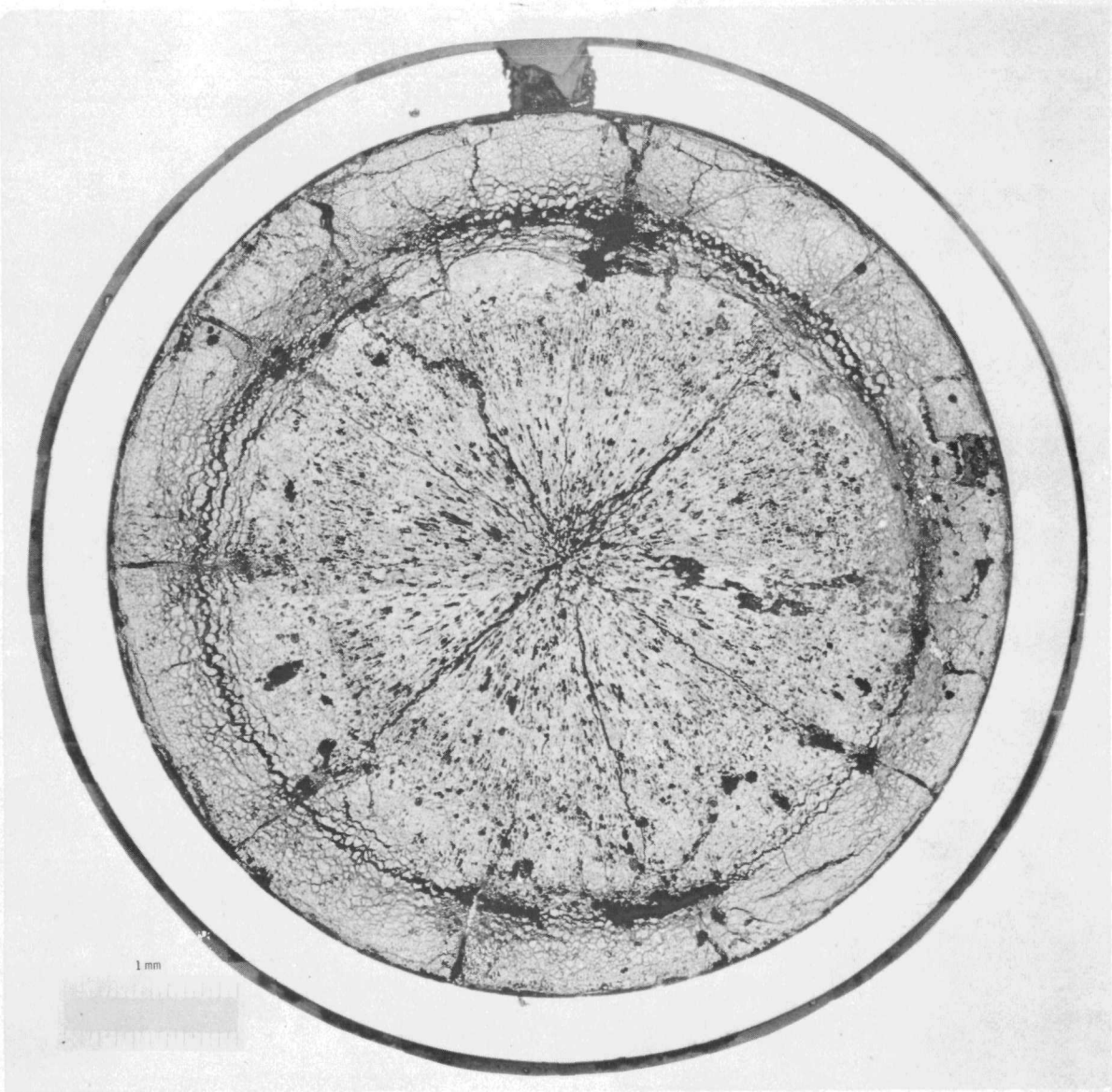

7711298

HEDL-ZP-8-24
Sample L
As Polished
1μ Diamond and Hyprez

FIGURE 19. Microstructure of Pin ZP-8-24, Section L.

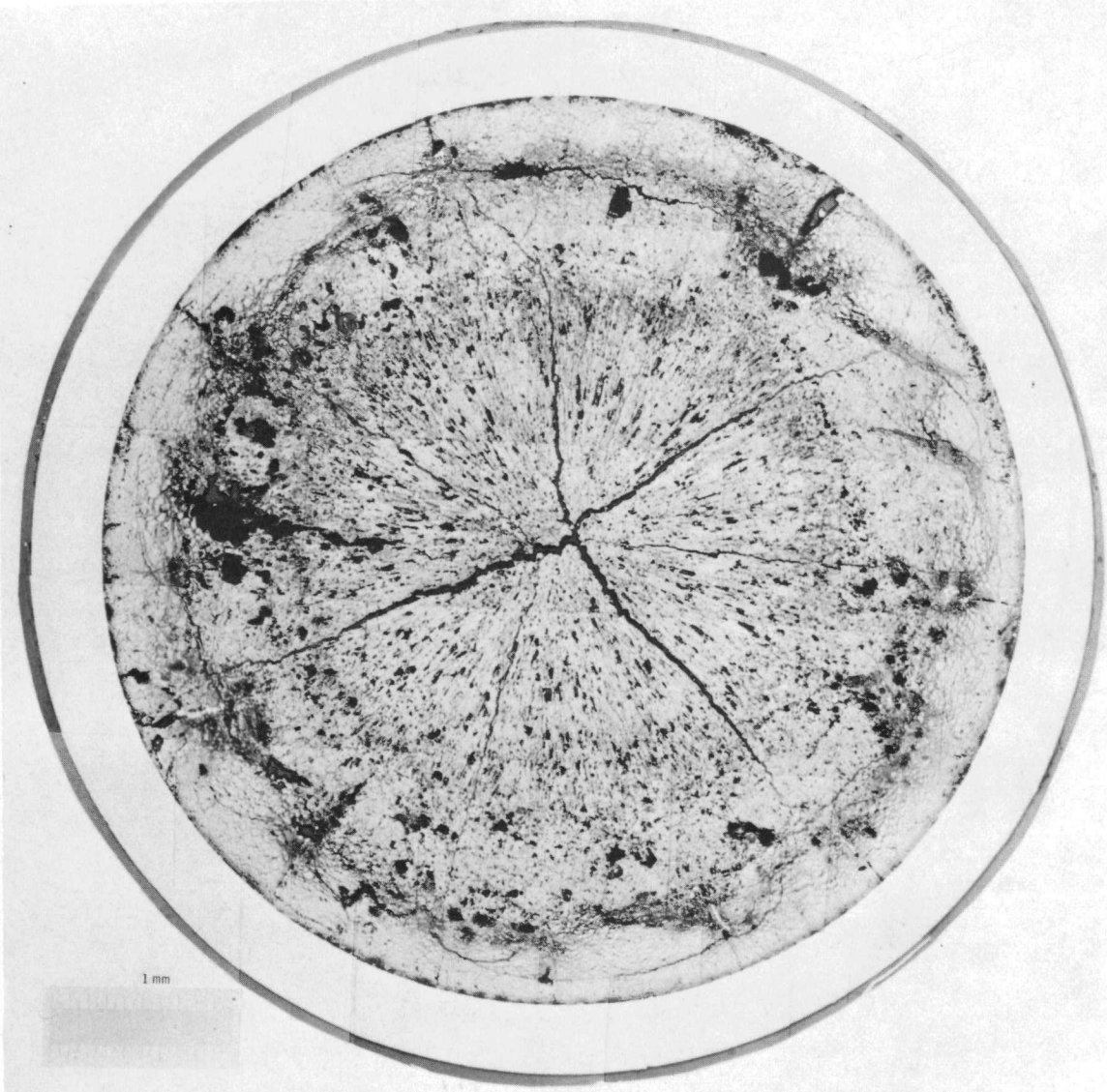

HEDL-ZP-8-24
Sample K
As Polished
1μ Diamond and Hyprez

FIGURE 20. Microstructure of Pin ZP-8-24, Section K.

MIXED OXIDE FUEL IRRADIATED IN EBR-II

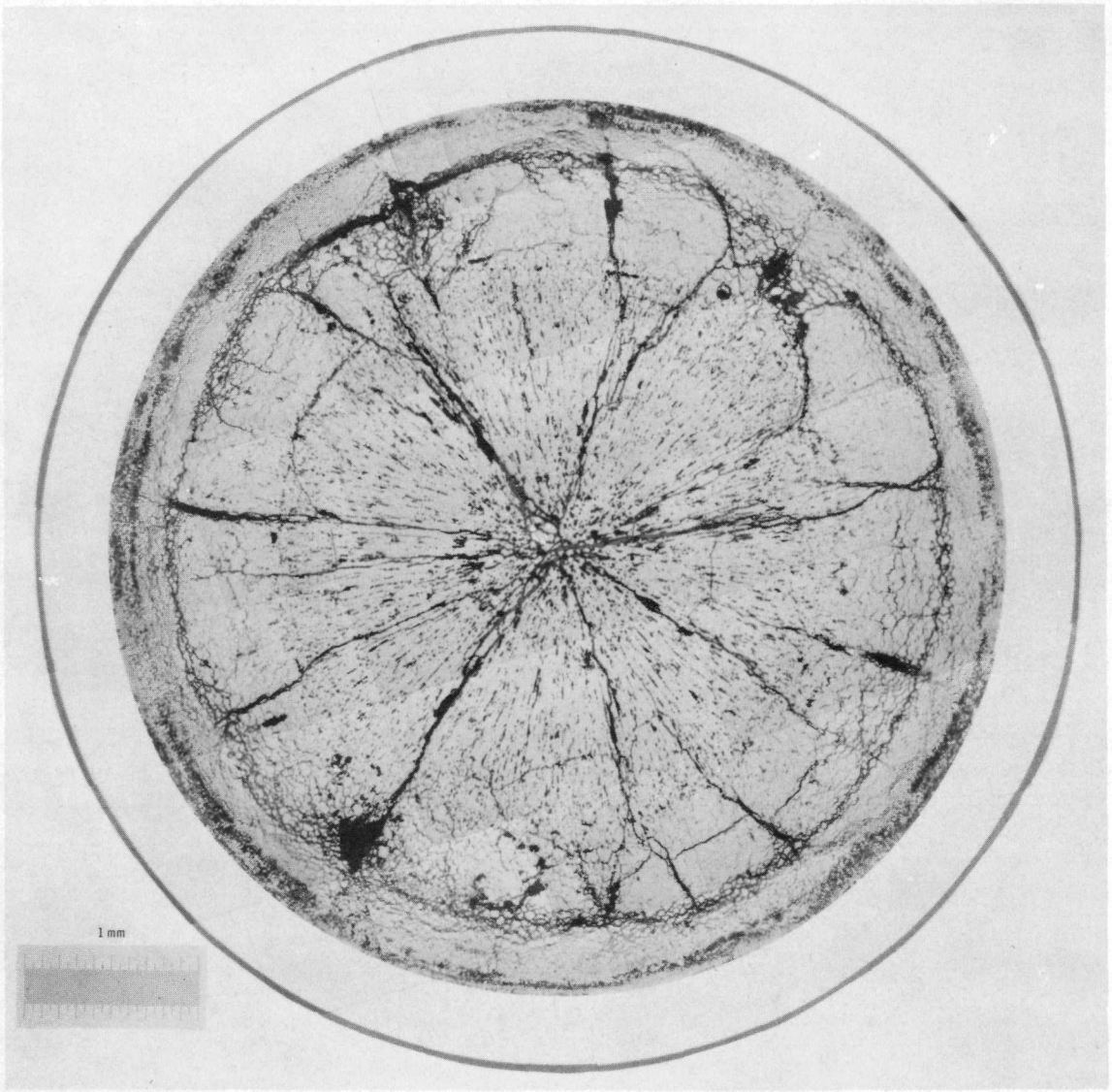

7711669

HEDL-ZP-8-24
Sample E
As Polished
1μ Diamond and Hyprez

FIGURE 21. Microstructure of Pin ZP-8-24, Section E.

MIXED OXIDE FUEL IRRADIATED IN EBR-II

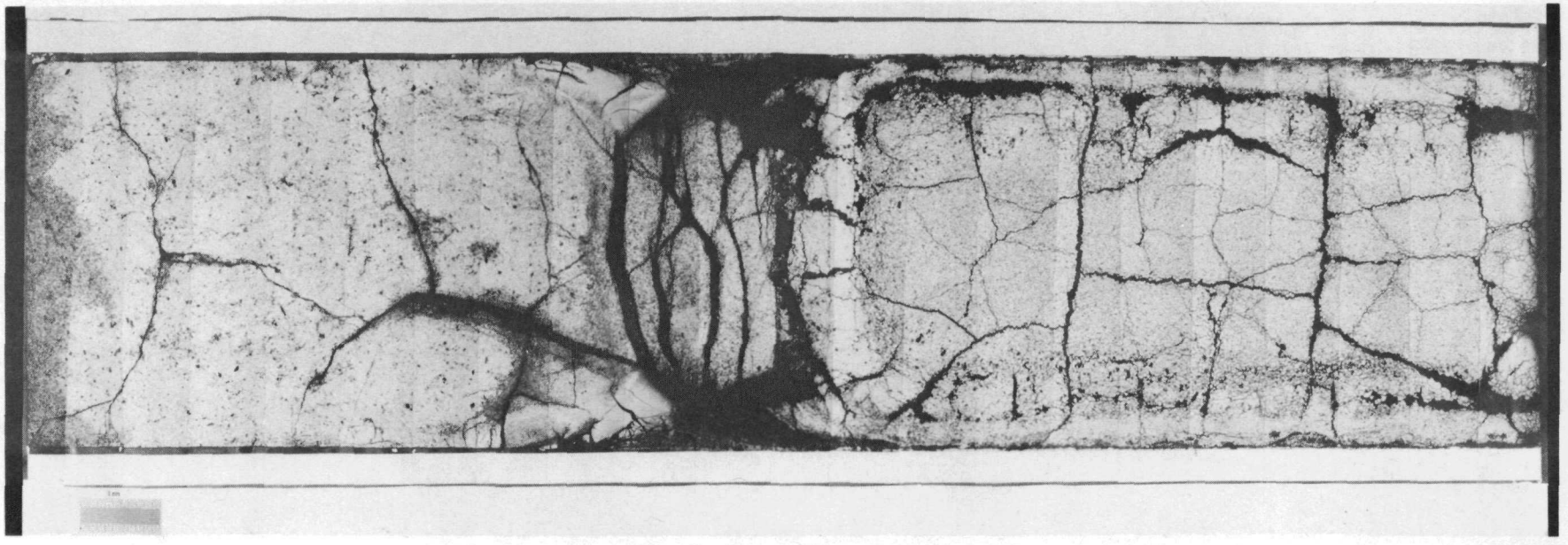

7711660

HEDL-ZP-8-24
Sample B
As Polished
1μ Diamond and Hyprez

FIGURE 22. Microstructure of Pin ZP-8-24, Section B.

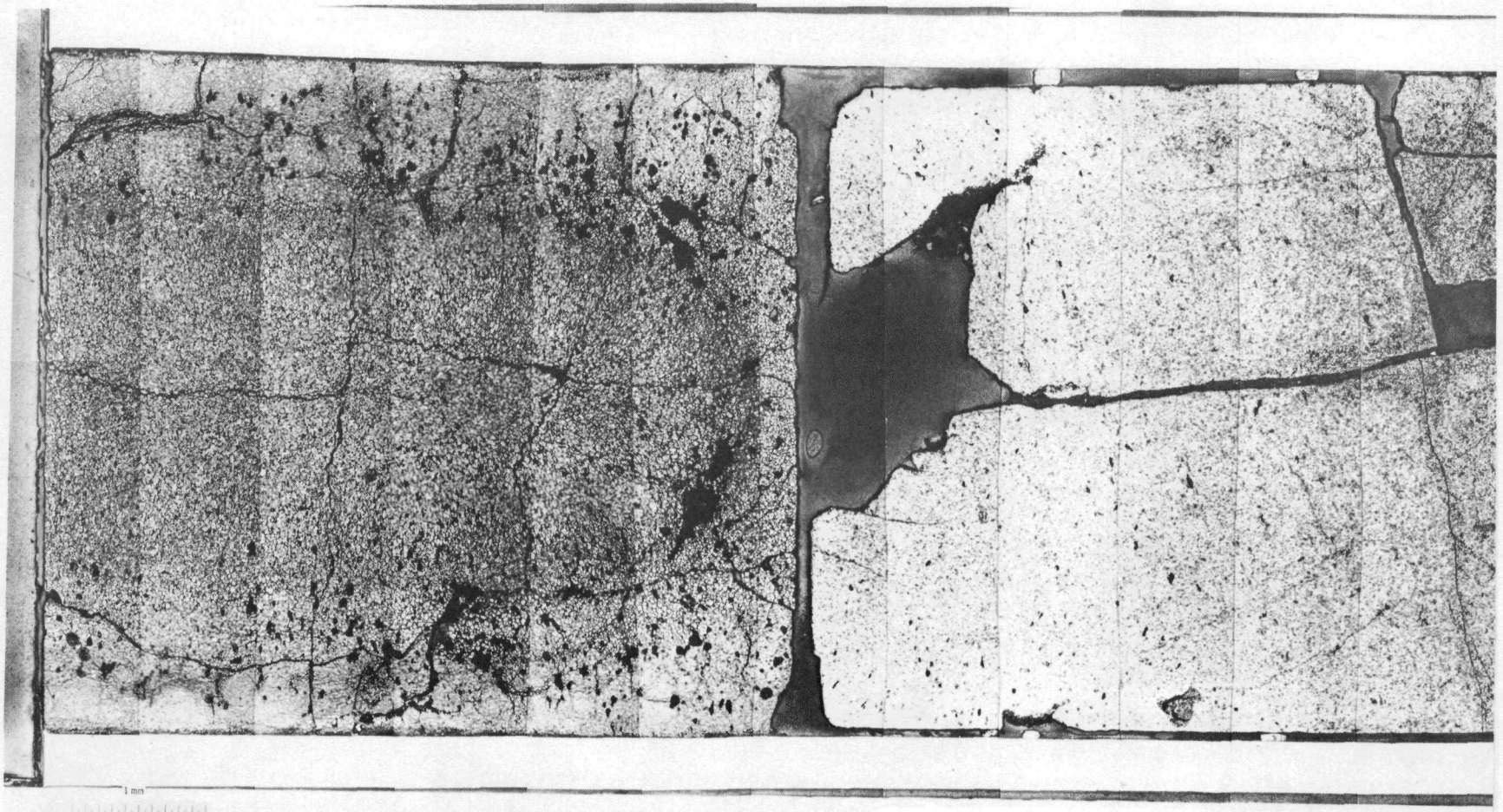

FIGURE 23. Microstructure of Pin ZP-8-24, Section P.

The characteristic appearance of the structure is shown in Figure 24. This figure, taken from the surface containing the slit extension, shows a reaction layer at the slit extension about 0.9-mm thick. Elsewhere around the circumference of the pin the reaction layer was 0.7-0.8 mm thick.

There was no visual evidence of sodium-UO_2 reaction in the insulator pellets although the fuel immediately adjacent to the insulators showed the same reaction product as fuel in the vicinity of the slit.

During fuel pin sectioning, the cladding density sample located at the bottom of the plenum region (280 mm or ∿11 inches above the top of the fuel) contained a small amount of foreign material. This material, which was dissolved in distilled water for gamma scan analysis, indicated the presence of ^{137}Cs, ^{134}Cs, and ^{125}Sb. Sodium with dissolved fission product cesium and antimony had moved from the fuel column into the upper plenum.

The surface through the lower slit extension (Figure 19, p. 36) was examined with the shielded electron microprobe. The grain boundary phase in the outer fuel rim (outside the circumferential cracking) was sodium-fuel reaction product. Semiquantitative analysis showed no segregation of plutonium from the fuel attributable to the chemical reaction, i.e., the ratio of x-ray intensities of uranium to plutonium in the fuel and in the sodium-fuel reaction product was 2.2 ±0.1. Radial cracks in the restructured zones (inside the circumferential cracking) contained sodium unreacted with fuel. These results indicate that sodium-fuel reaction was confined to the outer periphery of the fuel during irradiation and further sodium ingress occurred after termination of irradiation.

The destructive examination of the fuel pin was completed with the observation of typical irradiated microstructure in the AISI Type 316 SS 20% CW cladding. The slit extended intergranularly through the cladding.

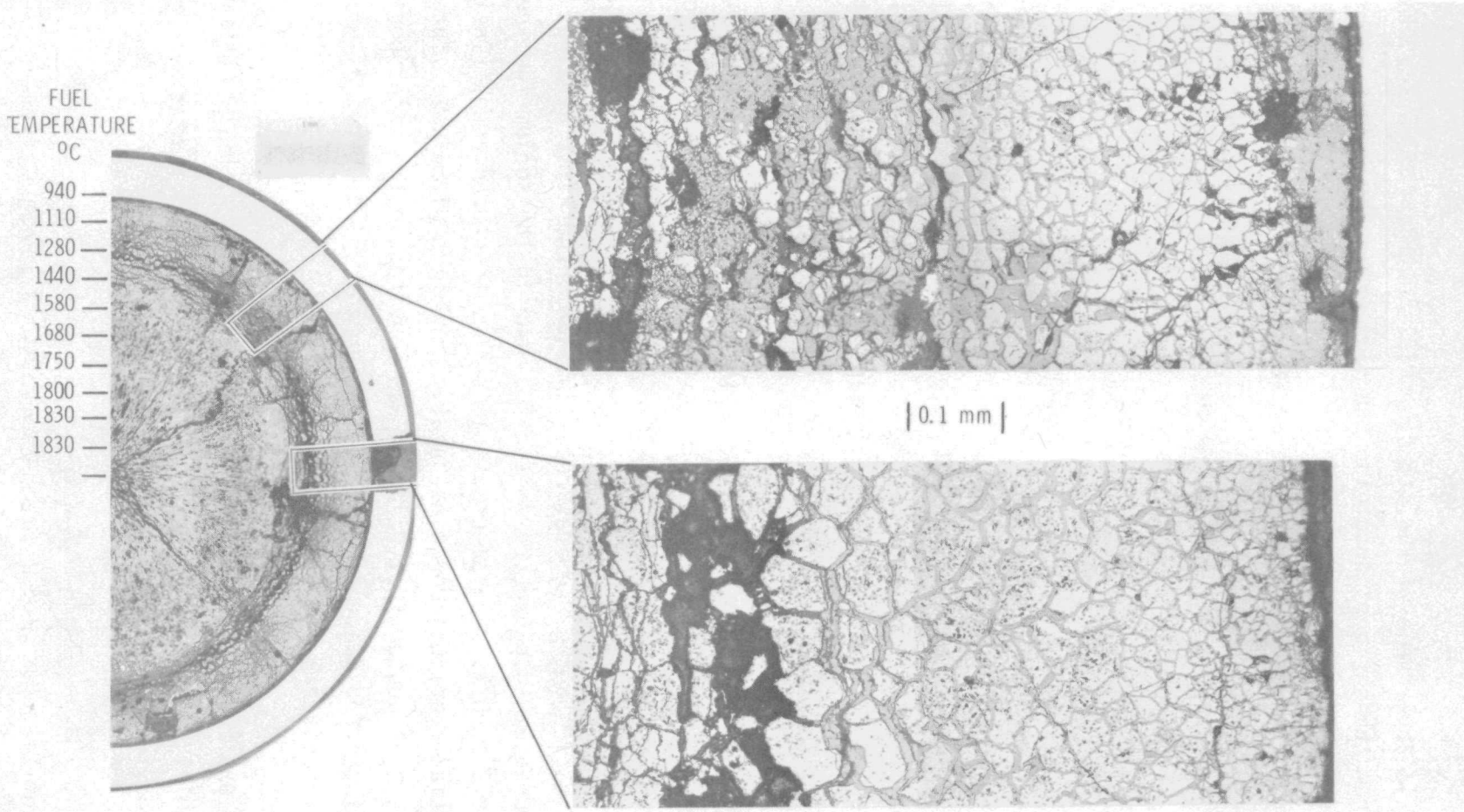

FIGURE 24. RBCB-6 Transverse Surface Through Lower Slit Extension. The appearance of the sodium-fuel reaction product under the slit extension is characteristic of the appearance away from the slit extension.

Scanning electron microscopy examination of one surface of the upper slit extension confirmed that the extension was intergranular. The surfaces of individual grains in the fracture showed distinct lattice-like features not generally observed in intergranular fracture (see Figure 25). The fracture surface also contained what appeared to be intergranular cracks between the grains. This secondary cracking gives the impression that grains are about to fall out. The profuse intergranular cracking may be indicative of a fracture process that is environmentally assisted.

The fine geometric patterns observed on the surface of numerous grains may be crystallographic in origin. The pattern spacing is of the same order of magnitude as the carbide-decorated slip traces determined from cladding metallography samples. The time when the geometric pattern developed is not clear; however, it is believed to have developed to a limited extent in the reactor and then developed further after removal from the reactor.

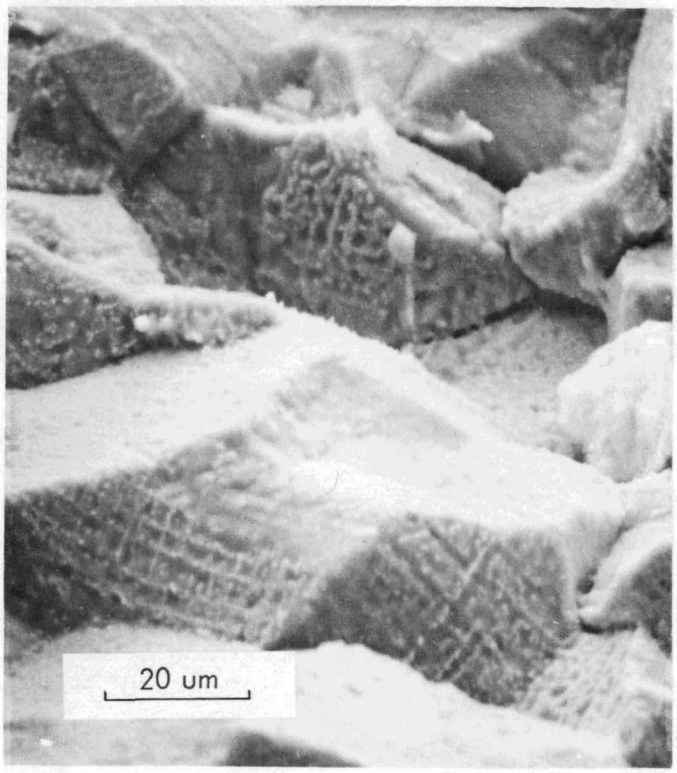

FIGURE 25. Lattice-Like Pattern on Grain Surfaces in Upper Slit Extension in Pin ZP-8-24 Cladding.

I. VOLUME-FRACTION REACTION PRODUCTS

Sodium-fuel reaction has been observed in laboratory tests and in tests conducted in-reactor with encapsulated fuel.[9] These tests suggest that the extent of fuel pin swelling is associated with the volume of sodium-fuel reaction product. Characterization of the volume fraction of reaction product establishes a basis for comparing the results of unencapsulated, in-reactor RBCB tests where pin swelling and reaction-product formation have occurred.

Fuel pin swelling is an important consideration in reactor safety analyses because excessive swelling can reduce coolant flow and result in a temperature increase in the coolant and consequently in the fuel pin(s) adjacent to the affected coolant channel(s). For this reason, it is important to establish that swelling is not excessive.

A maximum fuel pin diameter is approached when the reaction ceases because one of the reactants is consumed or because the temperature drops below a threshold value. A correlation between fuel pin swelling and volume of reaction product will lead to an estimate of maximum fuel pin swelling.

The volume fraction of sodium-fuel reaction product was estimated by point counting. In this method a regular grid is placed over a micrograph and the number of intersections of the grid that lie in the constituent of interest are counted. The areal fraction of the constituent in the microstructure is equal to the ratio of the number of intersections lying in the constituent to the total number of intersections in the area of interest. If the structure is isotropic, the areal fraction is equal to the volume fraction; for this analysis, isotropy is assumed.

The point-counting method employed used a 30 lines/inch grid. The grid was overlayed with a circle divided into 10° sectors and 0.2-in. wide annuluses. The grid and overlay were placed over a 75X photomosaic of the circular cross section. The 10° sectors in the cross section were characterized as containing

uniformly distributed reaction product and radially cracked or circumferentially cracked fuel with nonuniformly distributed reaction product. Several of the sectors in each category were point-counted to determine the fraction of reaction product; the remaining sectors were estimated based on the results.

Radial distributions of reaction product for the three transverse sections are shown in Figure 26. These distributions were obtained by averaging the sector values for each of the 0.2-in. wide annuluses. Figure 26 also shows the calculated fuel temperatures for each of the sections. These temperatures were calculated without adjusting the fuel or gap thermal conductivity for the presence of sodium-fuel reaction product.

The results shown in Figure 26 indicate a decrease in reaction product volume as the distance from the slit increases. Presumably this reflects the decreasing availability of sodium to continue the reaction. In each of the cross sections there is a well-defined boundary separating the region with sodium-fuel reaction from the region without reaction. In Section L (the section through the slit extension) the calculated temperature at the boundary is about 1325°C. In Section K the temperature at the boundary is about 1225°C, and in Section E it is about 1150°C. The different temperatures associated with reaction termination may result from not accounting for sodium-fuel reaction product in the temperature calculations or from the accessibility of sodium. Hopefully, additional RBCB tests will aid in defining temperature limits for the sodium-fuel reaction.

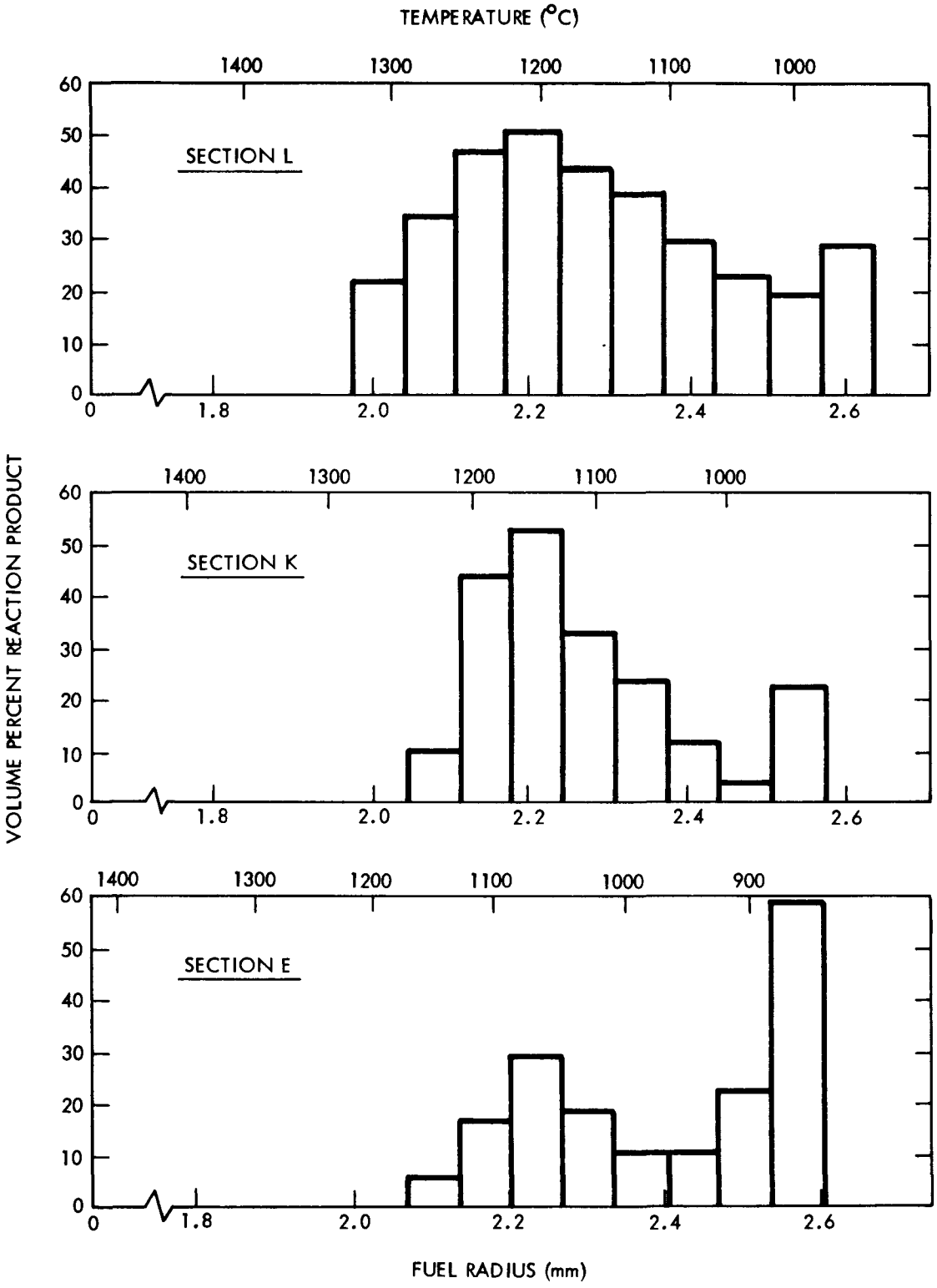

FIGURE 26. Radial Profile of Sodium-Fuel Reaction Product in RBCB-6 Fuel Pin ZP-8-24.

VI. DISCUSSION

Irradiation of RBCB-6 demonstrated that mixed-oxide fuel exposed to sodium coolant is easily monitored by DN detectors. Moreover, the test demonstrated that fuel pin degradation due to sodium-fuel reaction is a slow process and that reactor operators would have adequate time to take action before a safety hazard developed.

The mechanism of DN precursor release was not evident from this test. The nonlinear increase of DN signal with fuel pin power indicates that DN precursor release is not solely by a recoil mechanism. Fission product release by recoil would be linear with power since it would be proportional to fission rate.

The gradual increase in DN signal at full power is attributed to the growth of cladding cracks at both ends of the slit. The driving force of these slit extensions is the sodium-fuel reaction. With longer irradiation time, the slit would continue to extend in the downward direction. The extension in the upward direction would stop at the top of the fuel column since the upper UO_2 insulator did not react with sodium.

The maximum attainable slit width is also controlled by the extent of sodium-fuel reaction. This fuel pin did not show evidence that the reaction had reached completion at any axial height. Presumably longer irradiation time would have resulted in a larger pin diameter and a wider slit. If the available oxygen in the fuel were consumed, the sodium-fuel reaction would cease and the pin condition would remain stable.

There was no indication (visual or from the fissile assay) of fuel loss from the RBCB-6 fuel pin; however, this may be due in part to the relatively short irradiation time. These results do suggest that the sodium-fuel reaction product has sufficient structural integrity to allow longer irradiation without excessive fuel loss either in-reactor or during subsequent handling.

All of the test results indicated that the DN signal limit for test termination could be increased. Moreover, it was demonstrated that the DN signal was related to cladding defect area and that a larger defect area could be tolerated both from a reactor safety standpoint and a fuel handling standpoint. Further tests covering a range of fuel pin conditions will be required before a maximum tolerable DN signal limit can be established. It will also be important to compare results from fuel pins with machined defects with those from naturally occurring defects to insure the validity of these results.

VII. CONCLUSIONS

The RBCB-6 test results justify an increase in the DN signal limit for future RBCB tests. These tests provided evidence that

- DN signals are sensitive to cladding defect size.
- Cladding crack extension is slow enough that reactor operators can take appropriate action before a safety hazard arises.
- Fuel pin diameter increases cannot impair subassembly performance without an increase in DN signal because an increase in cladding defect size will accompany such a diameter increase.
- Fuel and fission product loss does not occur at an intolerable rate.

Additional RBCB tests are planned for EBR-II to establish a maximum acceptable DN signal limit.

VIII. REFERENCES

1. R. Monson et al., "Fission Product Control at EBR-II," Trans. ANS (27), 1977, pp. 822-823.

2. J. I. Sackett et al., "Preparations at EBR-II for Breached Element Operation," Trans. ANS (27), 1977, pp. 823-825.

3. R. V. Strain et al., "Design and Use of the Fission Product Source at EBR-II," Trans. ANS (27), 1977, pp. 825-826.

4. R. M. Fryer et al., "Safety-Related Questions for Operation with Defected Elements in EBR-II," Proceedings, Fast Reactor Safety and Related Physics, November 1976.

5. D. F. Washburn et al., "Mixed-Oxide Run-Beyond-Cladding-Breach Tests in EBR-II," Proceedings, International Conference on Fast Breeder Reactor Fuel Performance, March 1979, pp. 100-111.

6. J. D. Berger, "High-Speed Slitter for Irradiated Stainless-Steel Tubing," Trans. ANS (27), 1977, pp. 985-987.

7. R. G. Brown, Analysis of Heat Generating Blockages in CRBR Fuel and Radial Blanket Assemblies to Determine Detection Requirements, WARD-D-0119, September 1975.

8. E. E. Burdick, E. Fast, and D. W. Knight, The Advanced Reactivity Measurement Facilities - A Description and Performance Evaluation, IDO-17005, Idaho National Engineering Laboratory, 1964.

9. E. A. Aitken et al., "Reactions of Sodium with Mixed Oxide Fuel," ANS Proceedings, Fast Reactor Fuel Element Technology, New Orleans, April 1971.